Mathematical Biosciences 326 (2020) 108372

Contents lists available at ScienceDirect

Mathematical Biosciences

journal homepage: www.elsevier.com/locate/mbs

Original Research Article

Global dynamics of healthy and cancer cells competing in the hematopoietic system

Morten Andersen [a,*], Hans C. Hasselbalch [b], Lasse Kjær [b], Vibe Skov [b], Johnny T. Ottesen [a]

[a] IMFUFA, Department of Science and Environment, Roskilde University, Denmark
[b] Department of Haematology, Zealand University Hospital, Roskilde, Denmark

ABSTRACT

Stem cells in the bone marrow differentiate to ultimately become mature, functioning blood cells through a tightly regulated process (hematopoiesis) including a stem cell niche interaction and feedback through the immune system. Mutations in a hematopoietic stem cell can create a cancer stem cell leading to a less controlled production of malfunctioning cells in the hematopoietic system. This was mathematically modelled by Andersen et al. (2017) including the dynamic variables: healthy and cancer stem cells and mature cells, dead cells and an immune system response. Here, we apply a quasi steady state approximation to this model to construct a two dimensional model with four algebraic equations denoted the simple cancitis model. The two dynamic variables are the clinically available quantities *JAK2V617F* allele burden and the number of white blood cells. The simple cancitis model represents the original model very well. Complete phase space analysis of the simple cancitis model is performed, including proving the existence and location of globally attracting steady states. Hence, parameter values from compartments of stem cells, mature cells and immune cells are directly linked to disease and treatment prognosis, showing the crucial importance of early intervention. The simple cancitis model allows for a complete analysis of the long term evolution of trajectories. In particular, the value of the self renewal of the hematopoietic stem cells divided by the self renewal of the cancer stem cells is found to be an important diagnostic marker and perturbing this parameter value at intervention allows the model to reproduce clinical data. Treatment at low cancer cell numbers allows returning to healthy blood production while the same intervention at a later disease stage can lead to eradication of healthy blood producing cells.

Assuming the total number of white blood cells is constant in the early cancer phase while the allele burden increases, a one dimensional model is suggested and explicitly solved, including parameters from all original compartments. The solution explicitly shows that exogenous inflammation promotes blood cancer when cancer stem cells reproduce more efficiently than hematopoietic stem cells.

1. Introduction

Production of blood cells is denoted hematopoiesis. In the bone marrow reside the hematopoietic stem cells (HSC) that differentiate through multiple cell divisions into mature cells (MC) such as neutrophils, platelets, and red blood cells [1]. The number of human HSC has been estimated to be of the order of 10^4–10^5 each dividing every 25th to 50th week [2,3]. An order of magnitude of 10^{11} mature blood cells are produced daily [4], corresponding to millions per second, equivalent to 10 kg per year [5]. Clearly, a tight regulation of blood cell production is crucial and disturbances to this regulation may be severe.

Mathematical modelling has a prominent role in the study of hematopoiesis and its disorders and may be addressed from various areas of applied mathematics such as ordinary differential equations (ODE) [6–10], partial differential equations (PDE) [11–13], delay differential equations [5,14] or stochastic models [15–18]. Böttcher et al. [19] investigate the replicative capacity of progenitors and differentiated cells and use an ODE-model to investigate the cellular ageing based on data for telomere lengths and discuss implications for chronic myeloid leukemia. This approach relies on a discrete age structure, whereas for example Doumic et al. [20] consider a continuous age structure including stem cell dynamics, naturally leading to a PDE-formulation. Ashcroft et al. [21] focus on stem cell dynamics and use stochastic modelling to investigate wild type and mutant stem cells migrating back and forth to the blood stream and calibrate the model based on murine data.

Mutations in the DNA of the stem cells may be uncritical for hematopoiesis (neutral/passenger mutations) or they may be critically disturbing (driver mutations), giving rise to blood cancer characterized by an overproduction of malfunctioning mature cells — so-called transformed cells, which increase the risk of thrombosis [22]. Of special interest is the *BCR-ABL1* kinase translocation (the Philadelphia chromosome) as a driver for chronic myeloid leukemia, which has been studied using mathematical modelling [23–34]. However, the focus of the present paper is the type of blood cancers denoted Philadelphia-negative myeloprofilerative neoplasms (MPNs) including essential thrombocytosis, polycythemia vera and primary myelofibrosis. These are stem cell disorders evolving on a time scale of years characterized by few acquired driver mutations, where *JAK2V617F* (*JAK2*) is the most common [35].

* Corresponding author.
E-mail address: moan@ruc.dk (M. Andersen).

https://doi.org/10.1016/j.mbs.2020.108372
Received 27 August 2019; Received in revised form 6 May 2020; Accepted 6 May 2020
Available online 19 May 2020
0025-5564/

Few previous studies have addressed mathematical modelling of human MPNs. Zhang et al. [36] recently investigated a model of MPNs with inflammation as a fixed, constant input. Andersen et al. [37] proposed a more comprehensive model of human MPN development that is the starting point for the present paper. *JAK2* mutated cells are explicitly included at stem cell and mature cell level. As dynamical variables we include hematopoietic and cancer stem cells that battle through a stem cell niche interaction, hematopoietic and cancer mature cells, dead cells and inflammation level. This allows for investigation of several intricate couplings: How does the population of hematopoietic and cancer stem cells evolve and interact and how does this depend on the remaining part of the system? Is cancer development aligned with development of increasing inflammation and vice versa, is increasing inflammation positively or negatively affecting cancer progression? Which mechanisms should be altered to stop further disease progression or ultimately cure the patient? The long term behaviour of trajectories is investigated by a thorough analysis of attractors of the system elucidating conditions and intervention strategies for cancer escape, elimination, or equilibrium. In [38] the model is extended with T-cell response. Here, we disregard this extension to allow for analytical investigation.

Section 2 presents the basic Cancitis model originally proposed in [37]. A useful quasi-steady state approximation appears in Section 2.1. In Section 2.2 the system is transformed into the clinically relevant variables and the equations are scaled and a comprehensive analysis of the topology of the dynamics is presented. The model is compared to data and discussed in Section 3 along with various intervention strategies derived from the analysis of the model. The structure of the transformed equations suggests that early cancer dynamics, with and without treatment, can be captured by an explicit solution controlled by a single, lumped parameter.

2. Mathematical model of coupled blood production, blood cancer and inflammation

Fig. 1 illustrates how hematopoiesis can be maintained on a systemic level. Hematopoietic stem cells, x_0, can self renew where a non-linear inhibitory feedback accounts for limited niche space, resources, and cytokine feedback. Stem cells may also differentiate through multiple steps (represented by amplification factor, A) to mature blood cells, x_1, here being exemplified by the white blood cells (neutrophils). Both cell types may die, and debris of the dead cells, a, is eliminated or recycled by the immune system, here lumped together in one compartment, s, typically represented by cytokines associated with the immune system activity such as IL-1β, IL-1Ra. Il-2R, IL-8, Il-10,IL-12 and C-reactive protein. Excess of dead cells leads to increased clearance by immune cells (red arrow). A need for extra or fewer mature blood cells is thus mediated through the immune system [37–39].

In case of a stem cell mutation such as *JAK2*, Fig. 1 may be expanded with a stem cell compartment of cancer stem cells, CSC (y_0), as well as mutated mature blood cells (y_1) which is seen in Fig. 2, with corresponding equations (1), introduced by Andersen et al. [37] inspired by the models of chronic myeloid leukemia by Dingli and Michor [40] and by Stiehl et al. [41].

The introduction of mutated cells implies a competition at stem cell level where the HSC and CSC compete for space and nutrients in the bone marrow niche. Hematopoietic stem cells are characterized by a self renewal rate, r_x, death rate, d_{x0}, and differentiation into progeny, a_x. An inhibitory feedback, $\phi_x(x_0, y_0)$, from the stem cell niche takes into account the limited space and nutrient supply and the competition between HSC and CSC. Inflammation stimulates self renewal of stem cells [42] which is motivated by death of mature healthy cells and provides a demand for replacement by new ones. Hence, the effective self renewal is chosen as $r_x\phi_x(x_0, y_0)s$. Finally, HSC may mutate to become CSC with rate r_m. The chance of mutation is believed to increase with inflammation [36,43–53] justifying an effective mutation rate being $r_m s$.

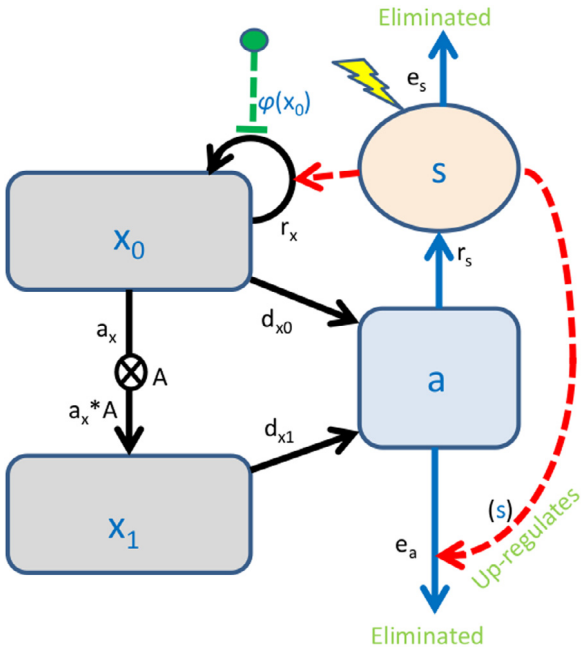

Fig. 1. Blood production in a healthy individual is regulated by hematopoietic stem cells (x_0) that self renew with rate r_x regulated by a stem cell niche feedback, $\phi(x_0)$ and cytokine feedback (red arrow from s compartment) or differentiate with rate a_x in multiple steps (illustrated by amplification A) to ultimately becoming hematopoietic mature cells (x_1). HSC die with rate d_{x0} and mature blood cells die with rate d_{x1}. Dead cells (a) are engulfed by the immune system that here is pooled together in one compartment (s) that stimulates clearing of dead cells with rate e_a. Presence of dead cells stimulates immune cells with rate r_s. Endotoxins, smoking and other environmental factors may add to the inflammatory response, thus we add such a term (characterized by the lightning symbol).

Proliferating stem cells go through a sequence of cell divisions to ultimately become mature, differentiated cells. As we do not account for all intermediate division steps, the growth rate of mature blood cells is a_x multiplied with amplification factor, A_x. The mature cells undergo apoptosis with rate d_{x_1}. Differential equations for CSC and cancer mature cells are described similar to their healthy counterparts.

The apoptosis compartment is a collection of all cells that have undergone apoptosis and is therefore positively stimulated by cells from other compartments with this destiny and negatively affected by clearing by the immune cells, which is happening through a second order mechanism — dead cells encountering immune cells are eliminated with a second order rate e_a.

The immune system activity level is exemplified by cytokines such as IL 6 or IL 8 that are inflammation markers related to hematological malignancies [46]. The complexity of the immune system is assumed to be simplified due to a fast immune response compared to the remaining dynamics resulting in a single, dynamical variable, s.

The immune level activity is stimulated by the presence of dead cells and has a self elimination proportional to the population size. Further, an exogenous immune stimulation is possible through $I(t)$ such as microbial infection and inflammation (e.g. smoking and pollution). The resulting differential equations are shown in (1).

$$x_0' = \left(r_x\phi_x s - d_{x0} - a_x\right)x_0 - r_m s x_0 \tag{1a}$$

$$x_1' = a_x A_x x_0 - d_{x1}x_1 \tag{1b}$$

$$y_0' = \left(r_y\phi_y s - d_{y0} - a_y\right)y_0 + r_m s x_0 \tag{1c}$$

$$y_1' = a_y A_y y_0 - d_{y1}y_1 \tag{1d}$$

$$a' = d_{x0}x_0 + d_{y0}y_0 + d_{x1}x_1 + d_{y1}y_1 - e_a a s \tag{1e}$$

$$s' = r_s a - e_s s + I(t) \tag{1f}$$

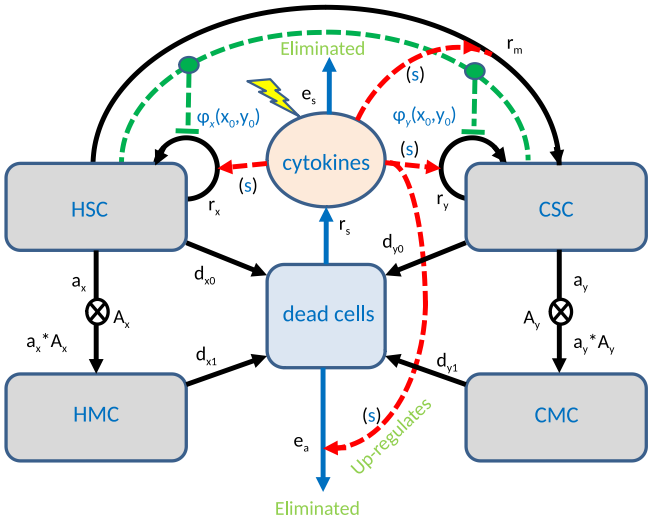

Fig. 2. The hematopoiesis-cancer-inflammation model consists of six cell populations; the hematopoietic stem cells (HSC), the hematopoietic mature cells (HMC), the cancer stem cells (CSC), and the cancer mature cells (CMC), dead cells and cytokines. The mechanisms described in Fig. 1 are included also for cancer cells. HSC mutates with rate r_m to become CSC. The stem cell niche feedbacks, ϕ_x and ϕ_y now depend on both CSC and HSC to comply with the competition for space and growth signals.

$$\phi_x = \phi_x(x_0, y_0) = \frac{1}{1 + \left(c_{xx}x_0 + c_{xy}y_0\right)^2} \tag{1g}$$

$$\phi_y = \phi_x(x_0, y_0) = \frac{1}{1 + \left(c_{yx}x_0 + c_{yy}y_0\right)^2}\,. \tag{1h}$$

As the model is inspired by Dingli and Michor [40], the default parameter values should be comparable to theirs. The cell numbers are chosen as typical numbers for a human. Prior to the first cancer stem cell, the model should be in steady state with 10^{10} mature blood cells (the neutrophil count, similar approach as in [41]), and 10^4 HSC which is a compromise between different reported values [40,41,54–56]. For a lifetime of one week in tissue, we chose $d_{x1} = 0.1$ per day [57]. The effective self renewal of stem cells $r_x\phi_x s$ is chosen to match cell division once per year.

The inflammatory level, s, is an abstract, scalable quantity whose progression which correlate with the inflammation markers IL-1β, IL-1Ra. Il-2R, IL-8, Il-10, IL-12 and C-reactive protein. Production of dead cells is correlated with plasma lactic dehydrogenase, see [37] including supplementary material for further details.

We expect $r_y > r_x$ for a blood cancer to develop, typically of measurable size after 5–10 years. For simplicity, we let unknown cancer cell parameter values equal their healthy counterpart. To satisfy the above conditions, the default parameter values in Table 1 are obtained. For further details on parameter estimation for this model, see [37].

The mutant rate is set to default value $2 \cdot 10^{-8}$ such that expansion of CSC is driven by mutations for CSC-values less than 1 and the CSC expansion is dominated by self renewal for CSC larger than 1. As the mutation rate increases with inflammation [58,59] the effective mutation rate is included as $r_m s$. In the further analysis we both investigate the effect of a continuous mutation corresponding to $r_m > 0$ and to a single event mutation corresponding to initializing the model with a single cancer cell but letting $r_m = 0$.

2.1. The simple cancitis model

The dynamics of cytokine regulation is fast compared to blood production [25]. Furthermore, white blood cells in the blood stream have a lifetime of six hours [60] to a week [57], while hematopoietic stem cells divide about once per year [61]. Therefore, we insist on

Table 1
Default parameter values of model (1) given as total cells per human (a male of weight 70 kg).

Parameter	Value	Unit	Parameter	Value	Unit
r_x	$8.7 \cdot 10^{-4}$	day^{-1}	r_y	$1.3 \cdot 10^{-3}$	day^{-1}
a_x	$1.1 \cdot 10^{-5}$	day^{-1}	a_y	$1.1 \cdot 10^{-5}$	day^{-1}
A_x	$3.7 \cdot 10^{10}$	–	A_y	$3.7 \cdot 10^{10}$	–
d_{x_0}	$2 \cdot 10^{-3}$	day^{-1}	d_{y_0}	$2 \cdot 10^{-3}$	day^{-1}
d_{x_1}	0.1	day^{-1}	d_{y_1}	0.1	day^{-1}
c_{xx}	$7.5 \cdot 10^{-5}$	–	c_{yy}	$7.5 \cdot 10^{-5}$	–
c_{xy}	c_{xx}	–	c_{yx}	c_{yy}	–
e_s	2	day^{-1}	r_s	$3 \cdot 10^{-4}$	day^{-1}
e_a	$1.6 \cdot 10^6$	day^{-1}	I	7	day^{-1}
r_m	0 or $2 \cdot 10^{-8}$	day^{-1}			

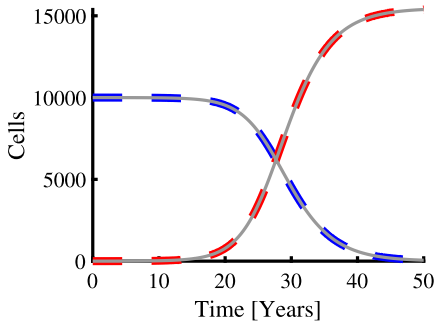

Fig. 3. Comparison of the full model (1) and the simple model (3) using default parameter values. Blue curve is the number of hematopoietic stem cells, red curve is number of cancer stem cells using the full model. Grey curves are the corresponding quantities in the reduced model.

mature cells and immune cells to be quickly equilibrated with the stem cell dynamics leading to the quasi steady state assumption

$$x_1' = y_1' = a' = s' = 0\,, \tag{2}$$

and with constant I making the system autonomous.

This leads to a two dimensional coupled ode-system, the *simple Cancitis model* (see the Appendix for detailed derivation)

$$x_0' = \left(r_x\phi_x s - d_{x0} - a_x\right)x_0 - r_m s x_0 \tag{3a}$$

$$y_0' = \left(r_y\phi_y s - d_{y0} - a_y\right)y_0 + r_m s x_0 \tag{3b}$$

$$x_1 = \frac{a_x A_x}{d_{x1}}x_0 \tag{3c}$$

$$y_1 = \frac{a_y A_y}{d_{y1}}y_0 \tag{3d}$$

$$s = \frac{I}{2e_s} + \sqrt{\left(\frac{I}{2e_s}\right)^2 + \frac{r_s\left(a_x A_x + d_{x0}\right)}{e_a e_s}\left(x_0 + \frac{a_y A_y + d_{y0}}{a_x A_x + d_{x0}}y_0\right)} \tag{3e}$$

$$a = -\frac{I}{2r_s} + \frac{e_s}{r_s}\sqrt{\left(\frac{I}{2e_s}\right)^2 + \frac{r_s\left(a_x A_x + d_{x0}\right)}{e_a e_s}\left(x_0 + \frac{a_y A_y + d_{y0}}{a_x A_x + d_{x0}}y_0\right)} \tag{3f}$$

$$\phi_x = \phi_x(x_0, y_0) = \frac{1}{1 + \left(c_{xx}x_0 + c_{xy}y_0\right)^2} \tag{3g}$$

$$\phi_y = \phi_x(x_0, y_0) = \frac{1}{1 + \left(c_{yx}x_0 + c_{yy}y_0\right)^2}\,. \tag{3h}$$

Allowed initial values of (x_0, y_0) belong to $D_1 = \mathbb{R}^+ \cup \{0\} \times \mathbb{R}^+ \cup \{0\}$. The parameter values are non negative so D_1 is invariant to the flow defined by Eq. (3).

Using default parameter values, system (3) is an excellent approximation to system (1) — see Fig. 3. To test the robustness, parameter values and initial conditions are varied and 100 simulations were performed. All initial conditions and parameters (except r_x, d_{x1}, A_x, e_s) are chosen from a normal distribution with mean given by the default value and standard deviation being 25% of the default value. If a

negative value is sampled, then the value is discarded and a new sample is taken. The parameters r_x, d_{x1}, A_x, e_s are then chosen such that the system is initiated at the hematopoietic steady state for mutation rate $r_m = 0$ and no initial cancer cells present. The full model and the simple model are evaluated daily for 80 years. The difference for each variable, x_0, x_1, y_0, y_1, a, s is computed and normalized by the initial value except y_0 and y_1 which are normalized by their hematopoietic counterpart. The maximum distance is then computed as the maximum deviation i.e. using the L^∞ norm. Due to the normalization, the distance is a dimension free number. The distance is less than 0.004 for all variables for all simulations, which means there is no visual difference in plots such as observed in Fig. 3. Hence, the difference between the full and simple model scaled by the baseline value is at any point in time less than one percent so the reduced model is a good approximation to the full model in all investigated cases.

2.2. Reformulating the simple model using the total white blood cells and JAK2 allele burden

The simple model can be formulated as a closed system of x_1 and y_1 using the proportionality between x_0 and x_1 and between y_0 and y_1. Excluding $(x_1, y_1) = (0, 0)$ we can define the coordinate transformation $D_1 \setminus \{(0,0)\} \to \mathbb{R}^+ \times [0,1]$, $(x_1, y_1) \to (z_1, z_2)$ where $z_1 \in \mathbb{R}^+$ is the total number of white blood cells and $z_2 \in [0,1]$ is the *JAK2* allele burden. Thus we exclude the trivial possibility of having no mature cells corresponding to $z_1 = 0$.

$$z_1 = x_1 + y_1 \tag{4a}$$
$$z_2 = \frac{y_1}{x_1 + y_1} \tag{4b}$$

with inverse mapping

$$x_1 = z_1(1 - z_2) \tag{5a}$$
$$y_1 = z_1 z_2 \,. \tag{5b}$$

This means that the clinically, measurable quantities are explicitly modelled as the only dynamic variables. Some parameters are difficult to assess, so for simplicity some parameters of the healthy cells and the cancer cells are chosen to be equal. Following [37] we investigate the case with the constraints

$$a_x = a_y \tag{6a}$$
$$A_x = A_y \tag{6b}$$
$$d_{x0} = d_{y_0} \tag{6c}$$
$$d_{x1} = d_{y_1} \tag{6d}$$
$$c_{xx} = c_{yy} \,. \tag{6e}$$

An analysis relaxing Eq. (6) is omitted here due to the parsimonious principle and lack of data.

The equations of total number of white blood cells and allele burden from Eqs. (3) and (4a) then simplify to

$$z_1' = z_1 \left(\left(r_x + z_2 \left(r_y - r_x \right) \right) \tilde{\phi}\tilde{s} - d_{x0} - a_x \right) \tag{7a}$$
$$z_2' = \left(1 - z_2\right) \left(z_2 \left(r_y - r_x \right) \tilde{\phi} + r_m \right) \tilde{s} \tag{7b}$$
$$\tilde{\phi} = \frac{1}{1 + \left(c_{xx} \frac{d_{x1}}{a_x A_x} \right)^2 z_1^2} \tag{7c}$$
$$\tilde{s} = \frac{I}{2e_s} + \sqrt{\left(\frac{I}{2e_s} \right)^2 + \frac{d_{x_1}}{a_x A_x} \frac{r_s \left(a_x A_x + d_{x0} \right)}{e_a e_s} z_1} \,. \tag{7d}$$

Then hypotheses based on clinical data can be directly investigated in the model and vice versa that features in the model may give rise to hypotheses that may be tested from appropriate clinical data. We will study system (7) with $z_1 \geq 0$ and $0 \leq z_2 \leq 1$. In particular, we will allow $z_1 = 0$ in the subsequent analysis even though the coordinate transformation $(x_1, y_1) \leftrightarrow (z_1, z_2)$ is not defined here. The differential equations (7) can easily be defined for $z_1 = 0$, and the stability of fixed points on the line $z_1 = 0$ provides information on phase space for $z_1 > 0$ where the coordinate transformation is well defined.

For $z_2(0) \in [0; 1]$, $z_2(t)$ stays within this interval as $(1 - z_2)$ is a factor in z_2' and for $z_2 = 0$, $z_2' \geq 0$. From Eq. (7a) we see that $\tilde{\phi}\tilde{s}$ is going to 0 for z_1 approaching infinity implying there exists a number M such that for $z_1 > M$ then $\dot{z}_1 < 0$. For non negative initial conditions, $z_1(t)$ stays non negative (as $z_1 = 0$ is a z_1 null cline). Therefore, the compact set $[0, M] \times [0, 1]$ is an *attracting trapping region* for the system.

2.3. Scaled equations

A scaled form of Eq. (7) is now formulated to facilitate further analysis. We introduce a constant $\bar{z}$ (value to be determined) and a variable, Z_1, such that

$$z_1 = \bar{z} Z_1 \,. \tag{8}$$

Similarly, we introduce the dimensionless time τ by

$$t = \bar{t}\tau \,, \tag{9}$$

where $\bar{t}$ is a constant to be determined. Then, differential equations of Z_1 and z_2 can be formulated from Eqs. (8), (9) and (7) with the notation $\dot{z} = \frac{dz}{d\tau}$. From the chain rule and Eq. (8)

$$\dot{Z}_1 = \frac{\bar{t}}{\bar{z}} z_1' \,. \tag{10}$$

Inserting the expression for z_1' from Eq. (7a) along with Eq. (8) we obtain

$$\dot{Z}_1 = \bar{t} Z_1 \left(\left(r_x + z_2 \left(r_y - r_x \right) \right) \tilde{\phi}\tilde{s} - d_{x0} - a_x \right) \tag{11}$$

with

$$\tilde{\phi}\tilde{s} = \frac{I}{2e_s} \frac{1 + \sqrt{1 + 4e_s d_{x1} r_s \frac{a_x A_x + d_{x0}}{I^2 a_x A_x e_a} \bar{z} Z_1}}{1 + \left(\frac{c_{xx} d_{x1}}{a_x A_x} \right)^2 \bar{z}^2 Z_1^2} \tag{12}$$

To simplify the denominator, we choose

$$\bar{z} = \frac{a_x A_x}{c_{xx} d_{x1}} \tag{13}$$

denoting the lumped parameter expression in the numerator by β_1,

$$\beta_1 = 4 \frac{e_s r_s}{c_{xx} e_a I^2} \left(a_x A_x + d_{x0} \right) \,, \tag{14}$$

Eq. (11) becomes

$$\dot{Z}_1 = \bar{t} Z_1 \left(r_x \frac{I}{2e_s} \left(1 + z_2 \left(\frac{r_y}{r_x} - 1 \right) \right) \frac{1 + \sqrt{1 + \beta_1 Z_1}}{1 + Z_1^2} - d_{x0} - a_x \right) \,. \tag{15}$$

By choosing

$$\bar{t} = \frac{2e_s}{r_x I} \,, \tag{16}$$

the first term is simplified, and we may conveniently introduce two lumped parameters, β_2 and β_3 by

$$\beta_2 = \frac{r_y}{r_x} - 1 \tag{17a}$$
$$\beta_3 = 2 \frac{e_s}{r_x I} \left(d_{x0} + a_x \right) \,. \tag{17b}$$

For $\dot{z}_2$ the equation then becomes

$$\dot{z}_2 = \bar{t} z_2' = \left(1 - z_2\right) \frac{1 + \sqrt{1 + \beta_1 Z_1}}{1 + Z_1^2} \left(\beta_2 z_2 + \frac{r_m}{r_x} \left(1 + Z_1^2 \right) \right) \tag{18}$$

which suggests a fourth lumped parameters as

$$\beta_4 = \frac{r_m}{r_x} \,. \tag{19}$$

Table 2
Default parameter values of system (21).

β_1	β_2	β_3	β_4
0.16	0.48	1.32	$2.3 \cdot 10^{-5}$

In summary, we obtain the system

$$\dot{Z}_1 = Z_1\left(\left(1+\beta_2 z_2\right)\frac{1+\sqrt{1+\beta_1 Z_1}}{1+Z_1^2} - \beta_3\right) \tag{20a}$$

$$\dot{z}_2 = \left(1-z_2\right)\frac{1+\sqrt{1+\beta_1 Z_1}}{1+Z_1^2}\left(\beta_2 z_2 + \beta_4\left(1+Z_1^2\right)\right), \tag{20b}$$

with new parameters given by relations to the old ones

$$\beta_1 = 4\frac{e_s r_s}{c_{xx} e_a I^2}\left(a_x A_x + d_{x0}\right) \tag{21a}$$

$$\beta_2 = \frac{r_y}{r_x} - 1 \tag{21b}$$

$$\beta_3 = 2\frac{e_s}{r_x I}\left(d_{x0} + a_x\right) \tag{21c}$$

$$\beta_4 = \frac{r_m}{r_x}. \tag{21d}$$

Eqs. (20) describe the mature cells (Z_1) in reduced units (Eq. (8)) and allele burden (z_2) progression over time, with parameters related to stem cell, mature cell and immune system mechanisms. Parameters are constrained by $\beta_1, \beta_3 > 0$ and $\beta_4 \geq 0$ and $\beta_2 \geq -1$, with default parameter values in Table 2 computed from the default parameters of the full model, Table 1. The parameter β_2 is related solely to the stem cell compartments, with negative values if $r_x > r_y$ and positive values if $r_x < r_y$. The parameter β_4 is the mutation rate relative to the hematopoietic self renewal rate. The value of this parameter will also be investigated when equal to zero, to allow for a one hit mutation (by setting the initial condition to one cancer cell) instead of considering a continuous mutation rate. The parameters β_1 and β_3 provide nontrivial connections between original system parameters related to the immune cells, dead cells, stem cells and mature cells. β_3 is the product of two lumped parameters that are important for cell exhaustion namely a loss versus production term on stem cell level, $\frac{a_x+d_0}{r_x}$, and a loss versus production term at immune cell level, $\frac{e_s}{I}$.

Regarding β_1, the presence of $a_x A_x$ implies that an increase in proliferation signal increase the β_1-value. An increased strength of the niche feedback (increasing c_{xx}) leads to a decreased β_1. Except for c_{xx}, the original parameters entering β_1 relates to the value of apoptotic cells and immune cells for a given number of stem cells — see Eqs. (3e) and (3f), as a ratio between effects that increase a and s levels namely $\frac{r_s}{e_a e_s}\left(a_x A_x + d_{x0}\right)$ and $\left(\frac{I}{e_s}\right)^2$.

2.4. Phase space analysis

The reduction from six differential equations to two has several useful implications. The order of the phase space is reduced from six to two allowing visualizations using the phase plane giving an overview of trajectories for many initial conditions simultaneously. The two-dimensional dynamics is quite restricted since trajectories cannot cross as the existence and uniqueness theorem applies. In the reduced model, the parameters of the full system are grouped in the parameters $\beta_1, \ldots, \beta_4$ showing the minimum number of parameters giving a functional dependence on the original parameters that otherwise would have shown up as correlated. The simplicity of system (20) implies that significant analysis can be conducted which is the focus of the current section. To categorize the steady states satisfying $\dot{Z}_1 = \dot{z}_2 = 0$ we employ the following vocabulary:

- A *hematopoietic steady state* is defined as having $z_2 = 0$.
- A *cancer steady state* is defined as having $z_2 = 1$.
- A *co-existing steady state* is defined as having $0 < z_2 < 1$.

A cancer steady state always exists with value $(Z_1, z_2) = (0, 1)$. For $\beta_4 = 0$ also $(Z_1, z_2) = (0, 0)$ is a trivial steady state solution.

2.4.1. Analytic bound on trapping region

The existence of a trapping region is already established. An analytic expression of an upper bound of Z_1 at the trapping region boundary is formulated. Consider Eq. (20a) for $Z_1 \geq 1$ implying $0 < Z_1^{-1} \leq 1$,

$$\begin{aligned}\left(1+\beta_2 z_2\right)\frac{1+\sqrt{1+\beta_1 Z_1}}{1+Z_1^2} - \beta_3 &\leq \left(1+|\beta_2|\right)\frac{Z_1^{-1}+\sqrt{Z_1^{-2}+\beta_1 Z_1^{-1}}}{Z_1^{-1}+Z_1} - \beta_3 \\ &\leq \left(1+|\beta_2|\right)\frac{1+\sqrt{1+\beta_1}}{Z_1} - \beta_3 .\end{aligned} \tag{22}$$

Solving for Z_1 requiring the latter expression being negative, an upper bound on the trapping region in the Z_1 direction is obtained,

$$M_1 = \max\{1, \left(1+|\beta_2|\right)\frac{1+\sqrt{1+\beta_1}}{\beta_3}\} = \left(1+|\beta_2|\right)\frac{1+\sqrt{1+\beta_1}}{\beta_3}, \tag{23}$$

For $\beta_2 < 0$, $|1+\beta_2 z_2| \leq 1$, providing the smaller bound

$$M_2 = \max\{1, \frac{1+\sqrt{1+\beta_1}}{\beta_3}\}. \tag{24}$$

Hence, an attractive trapping region is $M_1 \times [0,1]$ for $\beta_2 > 0$ and $M_2 \times [0,1]$ for $\beta_2 < 0$. This implies that solutions initially located outside the trapping region are attracted to it, and any solution once in the trapping region will stay there. A consequence of this is that the trajectories exist globally in forward time [62].

The possible dynamics in bounded, two-dimensional flow is very limited as the only attractors are fixed points or limit cycles. We restate the Poincaré–Bendixon theorem as stated in for example [63].

Theorem 1 (*Poincaré–Bendixon*). *Given a system of ordinary differential equations* $\frac{dx}{dt} = F(x)$, *where* x *is two dimensional, let* $x(t)$ *represent a solution trajectory of the system which is bounded. Then either* $x(t)$ *converges as* $t \to \infty$ *to an equilibrium point of the system, or it converges to a periodic cycle.*

Remark 1. Due to index theory [64], any periodic solution in a two-dimensional phase space must have at least one fixed point in its interior. Therefore, if no coexistence steady states exist, then no limit cycles can exist. From monotonicity properties of Eq. (20b), $\dot{z}_2 = 0$ only allows for coexistence points and limit cycles if $\beta_2 < 0$ and $\beta_4 > 0$ i.e. if HSC self renewal dominates CSC self renewal and new CSC are continuously produced by mutations.

All steady state solutions are roots of a polynomial of at most fifth order which easily can be solved numerically using standard software. As an example, consider the nontrivial cancer steady state satisfying $z_2 = 1$ and Z_1 being the solution of

$$0 = \left(\left(1+\beta_2\right)\frac{1+\sqrt{1+\beta_1 Z_1}}{1+Z_1^2} - \beta_3\right) \tag{25}$$

corresponding to

$$\sqrt{1+\beta_1 Z_1} = \frac{\beta_3}{1+\beta_2}\left(1+Z_1^2\right). \tag{26}$$

Squaring this expression gives a fourth order polynomial.

$$0 = \left(\frac{\beta_3}{1+\beta_2}\right)^2 Z_1^4 + 2\left(\frac{\beta_3}{1+\beta_2}\right)^2 Z_1^2 - \beta_1 Z_1 + \left(\frac{\beta_3}{1+\beta_2}\right)^2 - 1. \tag{27}$$

All roots can then easily be computed numerically for a given set of parameter values. Then, the relevant, physiological solutions must be real, satisfy $Z_1 > 0$ and fulfil equation (26). This approach implies that all critical points can be numerically computed. The local stability of a steady state can then be computed by evaluating the eigenvalues

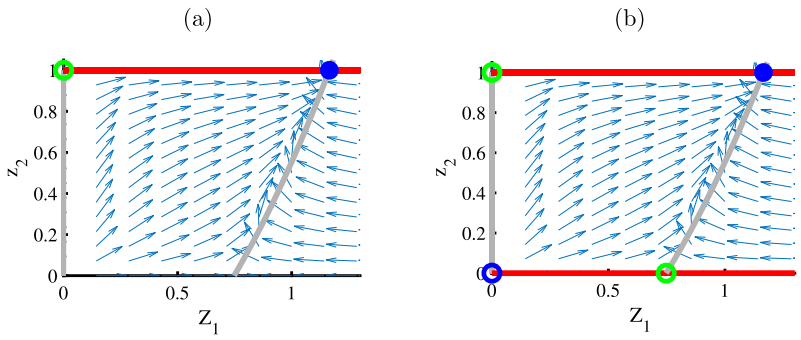

Fig. 4. Phase space of Eq. (20) for $\beta_2 > 0$. Open blue circles are unstable steady states with both eigenvalues having positive real part, green open circles are saddles, closed circles are stable steady states, grey curves are null clines of $\dot{Z}_1$, red curves are null clines of $\dot{z}_2$. Default parameters are used in (a) where a cancer steady state attracts all trajectories with $Z_1(0) > 0$, satisfying Lemma 1. In (b), default parameter values are used except $\beta_4 = 0$, so Lemma 2 applies showing a cancer steady state attracts trajectories with initial conditions $Z_1(0) > 0$ and $0 < z_2(0) < 1$.

of the Jacobian at the steady state, provided that the steady state is hyperbolic. Some phase planes corresponding to different parameter values are shown in Fig. 4. The following analysis addresses the typical phase plane topologies depending on the parameter values.

2.4.2. Hematopoiesis

We first consider hematopoiesis (Fig. 1) by expecting a stable, positive equilibrium of

$$\dot{Z}_1 = Z_1\left(\frac{1+\sqrt{1+\beta_1 Z_1}}{1+Z_1^2} - \beta_3\right). \tag{28}$$

Defining

$$F(Z_1) = \frac{1+\sqrt{1+\beta_1 Z_1}}{1+Z_1^2}, \tag{29}$$

a fixed point of $\dot{Z}_1$ for non zero Z_1 then requires $F(Z_1) - \beta_3 = 0$. The monotonicity properties of F are important for the further analysis. F is an increasing function of Z_1 for small, positive values, then it has a unique maximum at $Z_1 = \tilde{Z}_1$, and is decreasing for $Z_1 > \tilde{Z}_1$. $F(0) = 2$, and F goes to 0 for large Z_1. This implies that for $\beta_3 < 2$, a unique, positive solution exists to $F(Z_1) - \beta_3 = 0$. Since $F(0) - \beta_3 > 0$, then $F(Z_1) - \beta_3$ cross zero with negative slope so the steady state is stable [64].

For $2 < \beta_3 < F(\tilde{Z}_1)$ exactly two steady state positive solutions exist. The first steady state occurs where $F(Z_1) - \beta_3$ has positive slope, causing the steady state to be unstable, while the steady state with largest Z_1 value occurs where $F(Z_1) - \beta_3$ has negative slope, causing the steady state to be stable. For $\beta_3 > F(\tilde{Z}_1)$ no steady state solutions exist. A sufficient criterion for this is $\beta_3 > 1 + \sqrt{1+\beta_1^2}$. The parameter region allowing for two hematopoietic steady states is small. Biologically, an upper bound on β_3 is meaningful for hematopoiesis as stem cell exhaustion is expected for large parameters related to removal of cells, $(d_{x0} + a_x)e_s$ and small parameters related to production of cells, $r_x I$. For the remaining part of the paper, we will focus on $\beta_3 < 2$ as this guarantees existence of a stable fixed point of Eq. (28). For the default parameter values this criterion is fulfilled. For $\beta_3 < 2$ the unique, positive root of $F(Z_1) - \beta_3 = 0$ is denoted $\bar{Z}_1$, which has value 0.75 for default parameter values. An increase in β_1 shifts the equilibrium blood cell count to higher values and an increase in β_3 shifts the equilibrium blood cell to lower values as β_3 acts as an effective death rate of mature cells. In terms of original parameters this means that an increase in r_s or A_x increases the equilibrium blood cell number, while an increase in c_{xx} or e_a decreases the equilibrium blood cell number.

As $\dot{Z}_1 < 0$ for $Z_1 > \bar{Z}_1$, $[0; \bar{Z}_1] \times [0, 1]$ is a trapping region. We now systematically investigate the phase plane topologies of Eq. (20). When possible, the results are summarized in lemmas and phase plane figures, which may be conducted for a fast overview of the possible dynamics of the model.

2.4.3. The case $\beta_2 > 0$

Consider the case $\beta_2 > 0$ corresponding to $r_y > r_x$. First, we assume $\beta_4 > 0$, which prevents hematopoietic steady states since $\dot{z}_2 > 0$ for $z_2 = 0$. In this case, the only zero of $\dot{z}_2$ is for $z_2 = 1$ i.e. a cancer steady state, hence neither hematopoietic steady states nor coexistence points are possible for $\beta_2 > 0$, $\beta_4 > 0$. The criterion $\dot{Z}_1 = 0$ with $Z_1 \neq 0$ and $z_2 = 1$ is

$$0 = F(Z_1) - \frac{\beta_3}{1+\beta_2}, \tag{30}$$

which has a unique solution for $\beta_3 < 2$ by similar arguments as for the hematopoiesis investigation. Solutions to Eq. (30) solve

$$0 = \left(\frac{\beta_3}{1+\beta_2}\right)^2 Z_1^4 + 2\frac{\beta_3}{1+\beta_2}\left(\frac{\beta_3}{1+\beta_2} - 1\right) Z_1^2 - \beta_1 Z_1 + \frac{\beta_3}{1+\beta_2}\left(\frac{\beta_3}{1+\beta_2} - 2\right). \tag{31}$$

The first coefficient is positive and the third is negative. Hence, regardless of the sign of the second coefficient, there is one sign change from the first to the third coefficient. As $\beta_2 \geq 0$, $0 < \beta_3 < 2$ then $\frac{\beta_3}{1+\beta_2} - 2 \leq \beta_3 - 2 < 0$, hence the last term is negative, and the sequence of coefficients in Eq. (31) has one sign change for $\beta_2 \geq 0$ and $\beta_3 < 2$, so there is a unique solution to $\dot{Z}_1 = 0$ for $Z_1 > 0$ in this case. Denote this value by Z_1^*. In summary, for $\beta_2 \geq 0, \beta_4 > 0$ and $0 < \beta_3 < 2$ there are two fixed points: $(0, 1)$ and $(Z_1^*, 1)$.

Consider Eq. (20a) for any $z_2 \in [0; 1]$:

$$\lim_{Z_1 \to 0^+} \frac{\dot{Z}_1}{Z_1} = 2\left(1 + \beta_2 z_2\right) - \beta_3 \geq 2 - \beta_3 > 0. \tag{32}$$

This implies that the fixed point $(0, 1)$ is unstable and that we may choose any small $\epsilon > 0$ such that for $Z_1 = \epsilon$ then $\dot{Z}_1 > 0$ for any $z_2 \in [0; 1]$. The trapping region

$$T_1 = [\epsilon; M_1] \times [0; 1] \tag{33}$$

only contains one fixed point, namely $(Z_1^*, 1)$. As there can be no limit cycles, we have proved the following lemma.

Lemma 1. *For $\beta_2 \geq 0, \beta_4 > 0$ and $\beta_3 < 2$ there are two fixed points of Eq. (20), $(0, 1)$ and $(Z_1^*, 1)$. $(Z_1^*, 1)$ attracts all solutions with $Z_1(0) > 0$.*

For $\beta_2 > 0$ and $\beta_4 = 0$ there are additional two critical points, at $(0, 0)$ and the hematopoietic steady state $(\tilde{Z}_1, 0)$. As $\dot{z}_2 > 0$ for any $0 < z_2 < 1$ these two critical points are unstable. No coexistence points are possible. For any small $\epsilon > 0$ we define the set

$$T_2 = [\epsilon; M_1] \times [\epsilon; 1], \tag{34}$$

which is a trapping region. $(Z_1^*, 1)$ is the only attractor in T_2 and hence globally stable within T_2.

The line $z_2 = 0$ is invariant to the flow, and trajectories on this line are attracted to $(\tilde{Z}_1, 0)$ by similar reasoning as in Section 2.4.2.

Lemma 2. *For $\beta_2 > 0, \beta_4 = 0$ and $\beta_3 < 2$ there are four fixed points of Eq. (20), $(0,0)$, $(0,1)$, $(Z_1^*, 1)$, and $(\bar{Z}_1, 0)$. The cancer steady state $(Z_1^*, 1)$ attracts all solutions with $Z_1(0) > 0$, $z_2(0) > 0$. $(\bar{Z}_1, 0)$ attracts trajectories satisfying $z_2(0) = 0$ and $Z_1(0) > 0$.*

2.4.4. The case $\beta_2 = 0$ and $\beta_4 = 0$

Consider the case $\beta_2 = \beta_4 = 0$, $\beta_3 < 2$. The dynamics is very simple as $\dot{z}_2 = 0$ i.e. the allele burden does not vary with time. The dynamics of Z_1 then follows similar dynamics as for hematopoiesis, Section 2.4.2 i.e. there are two zeros of $\dot{Z}_1$, $Z_1 = 0$ and $Z_1 = \bar{Z}_1$. For any $Z_1(0) > 0$, Z_1 approaches $\bar{Z}_1$.

Disease progression occurs with $\beta_2 > 0$ leading to a measurable *JAK2* allele burden which may be altered by a targeted drug leading to $\beta_2 = 0$ i.e. similar HSC and CSC self renewal. In this case, the mature blood cell count will be maintained at a healthy value, with a constant proportion of *JAK2* cells.

2.4.5. The case $\beta_2 = 0$ and $\beta_4 > 0$

In this case $\dot{z}_2$ is only zero for $z_2 = 1$, and is increasing for $z_2 \in [0, 1)$. There are two steady states, $(0, 1)$ is unstable and $(\bar{Z}_1, 1)$ is stable and attracts all solutions with $Z_1(0) > 0$. This corresponds to the cancer stem cells dominate due to mutational supply from the hematopoietic stem cells.

2.4.6. The case $-1 < \beta_2 < 0$ and $\beta_4 = 0$

We investigate the case $-1 < \beta_2 < 0$ corresponding to $r_x > r_y$ and $\beta_4 = 0$ i.e no continuous mutation rate. Steady states are located at $(0, 1)$, $(\bar{Z}_1, 0)$, $(0, 1)$ and there may be additional two cancer steady states, related to the monotony properties of F. If $\frac{\beta_3}{1+\beta_2} < 2$ or $\frac{\beta_3}{1+\beta_2} = F(\tilde{Z})$ there are two cancer steady states. If $2 < \frac{\beta_3}{1+\beta_2} < F(\tilde{Z})$ there are three cancer steady states. If $\frac{\beta_3}{1+\beta_2} > F(\tilde{Z})$ there is only the trivial cancer steady state, $(0, 1)$, see Fig. 5.

The former case is symmetric to the case $\beta_2 > 0$, $\beta_4 = 0$. For any small $\epsilon > 0$ the set $[\epsilon; M_1] \times [0; 1 - \epsilon]$ is a trapping region, that only contains one steady state, which is on the boundary of the set.

In the remaining cases, $[0; M_1] \times [0; 1 - \epsilon]$ is a trapping region i.e. the flow is repelled from the cancer steady states. The trivial steady state $(0, 0)$ is a saddle, with stable manifold along the z_2 axis, which is also invariant to the flow. Hence, also in this case does $(\tilde{Z}, 0)$ attract initial conditions in $[\epsilon; M_1] \times [0; 1 - \epsilon]$.

Lemma 3. *For $-1 < \beta_2 < 0, \beta_4 = 0$ and $\beta_3 < 2$ the hematopoietic steady state $(\bar{Z}_1, 0)$ attracts all trajectories with $Z_1(0) > 0$, $z_2(0) < 1$. Unstable steady states are $(0, 0), (0, 1)$ and if $2 < \frac{\beta_3}{1+\beta_2} < F(\tilde{Z})$ there are additional two unstable cancer steady states.*

2.4.7. The case $-1 < \beta_2 < 0$ and $\beta_4 > 0$

In this case there are no hematopoietic steady states, as $\dot{z}_2 > 0$ for $z_2 = 0$. There may be zero, one or two cancer steady states, satisfying Eq. (30). Zeros of $\dot{z}_2$ are $z_2 = 1$ or $z_2 = f_1(Z_1)$ with

$$f_1(Z_1) = -\frac{\beta_4}{\beta_2}\left(1 + Z_1^2\right). \tag{35}$$

As f_1 is increasing with Z_1, we may use Eq. (24) to get an upper bound on this null cline within the Z_1 values of the trapping region. Then, f_1 has values in $[-\frac{\beta_4}{\beta_2}; -\frac{\beta_4}{\beta_2}\left(1 + \left(\frac{1+\sqrt{1+\beta_1}}{\beta_3}\right)^2\right)]$ within the Z_1 values of the trapping region.

The null clines of $\dot{Z}_1$ are $Z_1 = 0$ or $z_2 = f_2(Z_1)$ with

$$f_2(Z_1) = \frac{1}{-\beta_2}\left(1 - \frac{\beta_3}{F(Z_1)}\right). \tag{36}$$

For admissible z_2 values $1 > -\beta_2 > \beta_4 > 0$ is needed. The Jacobian evaluated at the steady state $(0, -\frac{\beta_4}{\beta_2})$ is then

$$J\left(0, -\frac{\beta_4}{\beta_2}\right) = \begin{bmatrix} 2\left(1-\beta_4\right) - \beta_3 & 0 \\ 0 & 2\beta_2\left(1 + \frac{\beta_4}{\beta_2}\right) \end{bmatrix}, \tag{37}$$

The second eigenvalue is always negative, with corresponding eigen direction being the z_2 axis. The sign of first eigenvalue $2\left(1-\beta_4\right) - \beta_3$ then determines the stability properties. By direct calculation, it is easily seen that the steady state is stable if $f_1(0) > f_2(0)$ and a saddle if $f_1(0) < f_2(0)$ thus proving the following remark.

Remark 2. A necessary condition for any coexistence steady state is $1 > -\beta_2 > \beta_4 > 0$. This condition is also sufficient for a coexistence point located at the boundary of the trapping region $(0, -\frac{\beta_4}{\beta_2})$. This steady state is a saddle with stable eigenvector along the z_2-axis if $2(1-\beta_4) - \beta_3 > 0$ (corresponding to $f_1(0) < f_2(0)$), and a stable node if $2(1-\beta_4) - \beta_3 < 0$ (corresponding to $f_1(0) > f_2(0)$).

A cancer steady state $(Z_1^*, 1)$ with positive Z_1^* must satisfy $f_2(Z_1^*) = 1$ which is equivalent to $F(Z_1^*) = \frac{\beta_3}{1+\beta_2}$. Linear stability analysis provides knowledge of the type of steady state based on f_1 and f_2 in the generic cases.

Lemma 4. *Let $-1 < \beta_2 < 0$, $\beta_4 > 0$, $0 < \beta_3 < 2$. If a cancer steady state exists with $f_2(Z_1^*) = 1$ it is*

- *a saddle if $f_2'(Z_1^*) > 0 \wedge f_1(Z_1^*) > 1$ or $f_2'(Z_1^*) < 0 \wedge f_1(Z_1^*) < 1$.*
- *an unstable node or focus if $f_2'(Z_1^*) > 0 \wedge f_1(Z_1^*) < 1$.*
- *a stable node or focus if $f_2'(Z_1^*) < 0 \wedge f_1(Z_1^*) > 1$.*

Proof. The proof is based on direct computation of the trace and determinant of the Jacobian evaluated at the steady state, providing knowledge of the eigenvalues. If the determinant is negative, the steady state is a saddle. If the determinant is positive and the trace is positive, the steady state is an unstable node or focus. If the determinant is positive and the trace is negative, the steady state is a stable node or focus.

$$\det\left(J\left(Z_1^*, 1\right)\right) = -\beta_2 Z_1^*\left(1+\beta_2\right) F'(Z_1^*) F(Z_1^*)\left(1 - f_1(Z_1^*)\right) \tag{38a}$$

$$tr\left(J\left(Z_1^*, 1\right)\right) = Z_1^*\left(1+\beta_2\right) F'\left(Z_1^*\right) - \beta_2 F\left(Z_1^*\right)\left(1 - f_1\left(Z_1^*\right)\right) \tag{38b}$$

As $\text{sign}(F'(Z_1^*)) = \text{sign}(f_2'(Z_1^*))$ the lemma follows directly. □

The cases not covered by the lemma require a nonlinear analysis and will not be pursued further.

A coexistence steady state is a point $(\hat{Z}_1, \hat{z}_2)$ satisfying $0 < f_1(\hat{Z}_1) = f_2(\hat{Z}_1) < 1$.

Lemma 5. *If a coexistence point $(\hat{Z}_1, \hat{z}_2)$ exists, then it is a saddle if $f_1'(\hat{Z}_1) < f_2'(\hat{Z}_1)$ and stable focus or a stable node if $f_1'(\hat{Z}_1) > f_2'(\hat{Z}_1)$ and $f_2'(\hat{Z}_1) < 0$.*

Proof. The proof is straight forward computation by evaluating the trace and determinant of the Jacobian evaluated at the steady state. Negative determinant implies a saddle, while a positive determinant together with negative trace implies both eigenvalues have negative real part meaning that the steady state is a stable node or a stable focus.

$$\det\left(J\left(\left(\hat{Z}_1, \hat{z}_2\right)\right)\right) = -\beta_2 \hat{Z}_1\left(1 - \hat{z}_2\right) F\left(\hat{Z}_1\right)\left(2\beta_4 \hat{Z}_1 F\left(\hat{Z}_1\right) - \frac{\beta_3 F'\left(\hat{Z}_1\right)}{F\left(\hat{Z}_1\right)}\right). \tag{39}$$

Then, notice that

$$f_1'\left(\hat{Z}_1\right) < f_2'\left(\hat{Z}_1\right) \Leftrightarrow 2\beta_4 \hat{Z}_1 F\left(\hat{Z}_1\right) - \frac{\beta_3 F'\left(\hat{Z}_1\right)}{F\left(\hat{Z}_1\right)} < 0 \tag{40}$$

proving that if $(\hat{Z}_1, \hat{z}_2)$ exists, then it is a saddle if $f_1'(\hat{Z}_1) < f_2'(\hat{Z}_1)$.

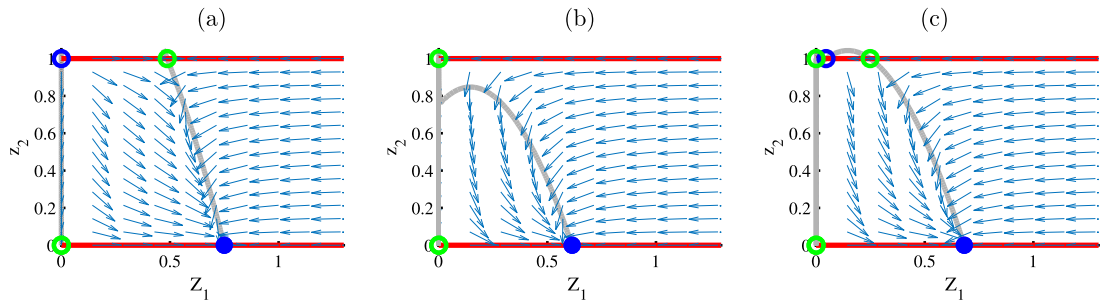

Fig. 5. Phase space for $-1 < \beta_2 < 0$, $\beta_4 = 0$. In all cases $(\bar{Z}_1, 0)$ attracts all trajectories excluding initial condition $Z_1(0) = 0$ or $z_2(0) = 1$.

Similarly, $\det\left(J\left((\hat{Z}_1, \hat{z}_2)\right)\right) > 0$ if $f_1'(\hat{Z}_1) > f_2'(\hat{Z}_1)$, hence eliminating saddle type fixed point. As

$$tr\left((\hat{Z}_1, \hat{z}_2)\right) = \beta_3 \hat{Z}_1 \frac{F'\left(\hat{Z}_1\right)}{F\left(\hat{Z}_1\right)} + \beta_2\left(1 - \hat{z}_2\right) F\left(\hat{Z}_1\right), \tag{41}$$

the trace is guaranteed to be negative if $F'\left(\hat{Z}_1\right) < 0$. Since

$$f_2'(Z_1) = \frac{\beta_3}{-\beta_2} \frac{F'(Z_1)}{F(Z_1)^2}, \tag{42}$$

then a sufficient criterion for negative trace is $f_2'\left(\hat{Z}_1\right) < 0$ proving the second part of the lemma. □

A case not covered in the lemma is $f_1'(\hat{Z}_1) > f_2'(\hat{Z}_1) \wedge f_2'(\hat{Z}_1) > 0$. We can rule out a saddle point, but the sign of the trace is not known. Perturbing a parameter such that the trace changes sign while $f_1'(\hat{Z}_1) > f_2'(\hat{Z}_1)$ prior and after perturbation implies that the real part of both eigenvalues shift sign at the same parameter value, suggesting a Hopf-bifurcation. This is indeed possible to observe in simulations though this requires an unrealistically large β_4 value, see Fig. 10.

Lemma 6. *If $f_2(\bar{Z}_1) > f_1(\bar{Z}_1)$ and $f_1(\bar{Z}_1) < 1$ then there exists a stable coexistence point $(\hat{Z}_1, \hat{z}_2)$ with $\tilde{Z}_1 < \hat{Z}_1 < \bar{Z}_1$ and $\hat{z}_2 < f_1(\bar{Z}_1)$ and there are no closed orbits enclosing $(\hat{Z}_1, \hat{z}_2)$.*

Proof. Recall that f_2 is strictly decreasing for $Z_1 > \tilde{Z}_1$ and $f_2(\bar{Z}_1) = 0$ and f_1 is strictly increasing. Hence, a unique intersection, $\left(\hat{Z}_1, f_1(\hat{Z}_1)\right)$, between f_1 and f_2 exists for a $\hat{Z}_1$ bounded above by $\bar{Z}_1$ and below by $\tilde{Z}_1$. As $0 < f_1(Z_1) < 1$ for $0 < Z_1 < \bar{Z}_1$, then $f_1(\hat{Z}_1) = \hat{z}_2 \in (0, 1)$. As $f_2'(\hat{Z}_1) < 0$ and $f_1'(\hat{Z}_1) > 0$ then $(\hat{Z}_1, \hat{z}_2)$ is a stable steady state by Lemma 5. To show there can be no closed orbits encircling $(\hat{Z}_1, \hat{z}_2)$, consider Fig. 6. The argument is based on showing existence of a continuum of invariant regions containing the steady state point. Notice that for $\tilde{Z} < Z_1 \leq \bar{Z}$ then f_2 is monotone and hence f_2^{-1} is well defined.

Any closed orbit encircling $(\hat{Z}_1, \hat{z}_2)$ must have an intersection $P = (p_1, p_2)$ with $z_2 = f_2(Z_1)$ for $Z_1 \in (\hat{Z}_1; \bar{Z}_1]$. Choosing a sufficiently small $\delta > 0$ we construct the box with corners $(p_1 + \delta, p_2)$, $(p_1 + \delta, f_2(p_1 + \delta) + \delta)$, $(f_2^{-1}(f_2(p_1 + \delta) + \delta) - \delta, f_2(p_1 + \delta) + \delta)$, $(f_2^{-1}(f_2(p_1 + \delta) + \delta) - \delta, p_2)$. Let the normal vector to the box be pointing outwards. Consider the line segment of the box spanned by $(p_1 + \delta, p_2)$, $(p_1 + \delta, f_2(p_1 + \delta) + \delta)$. As this line segment is to the right of the null cline of $\dot{Z}_1$, then $\dot{Z}_1 < 0$ everywhere on this line segment. As the outward normal of the box is $(1, 0)$ everywhere on this line segment, then $(\dot{Z}_1, \dot{z}_2) \cdot (1, 0) < 0$ showing the flow is pointing inwards to the box. By similar arguments, the flow is pointing inwards on the remaining three sides of the box, i.e the box is an invariant set. By existence and uniqueness at P the proposed closed orbit contains points both inside and outside the box region. However, any trajectory once in the box region cannot escape to reconnect at P from outside the box. Hence, there are no closed orbits encircling $(\hat{Z}_1, \hat{z}_2)$. □

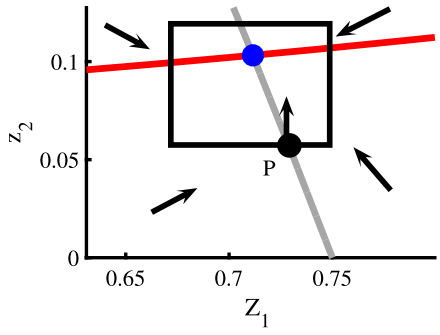

Fig. 6. Illustration of no limit cycle when the conditions of Lemma 6 are fulfilled. The red curve is the null cline of $\dot{z}_2$, grey curve is the null cline of Z_1. Any limit cycle must enclose a critical point and for the parameter constraints considered, there is exactly one coexistence steady state (blue dot). Therefore, any limit cycle must intersect the null cline of Z_1, denote such a point P. Construct a rectangular box as shown. At P the flow is along the z_2-axis hence pointing into the box. As the existence and uniqueness theorem applies, the trajectory through P consists of points both inside and outside of the box. However, the box is a trapping region as seen by inspection of the null clines and that $\dot{Z}_1$ and $\dot{z}_2$ are continuous in Z_1 and z_2. Therefore, the trajectory through P entering the box cannot escape it to reconnect with P from outside the box. Hence, there can be no limit cycle through P, and hence no limit cycle at all.

Remark 3. If $f_2(0) > f_1(\bar{Z})$ and $f_1(\bar{Z}) < 1$ then Lemma 6 is fulfilled and there is a unique coexistence point with positive Z_1 value. This out rules period solutions globally. A sufficient criterion for this is

$$\frac{1}{2}\left(2 - \beta_3\right) > \beta_4\left(1 + \left(\frac{1 + \sqrt{1 + \beta_1}}{\beta_3}\right)^2\right) \tag{43}$$

together with

$$1 > \beta_4\left(1 + \left(\frac{1 + \sqrt{1 + \beta_1}}{\beta_3}\right)^2\right). \tag{44}$$

If inequalities (43) and (44) are met then for sufficiently small $\epsilon > 0$ the set

$$T_3 = [\epsilon; M_1] \times [0; 1 - \epsilon] \tag{45}$$

is invariant to the flow, and the only steady state in T_3 is the coexistence steady state. By the Poincaré–Bendixon Theorem this point is then attracting all trajectories in T_3 i.e. the following lemma is proved

Lemma 7. *For $\beta_2 < 0, \beta_3 < 2, \beta_4 > 0$, $\frac{1}{2}\left(2 - \beta_3\right) > \beta_4\left(1 + \left(\frac{1+\sqrt{1+\beta_1}}{\beta_3}\right)^2\right)$, $1 > \beta_4\left(1 + \left(\frac{1+\sqrt{1+\beta_1}}{\beta_3}\right)^2\right)$ a unique, positive, coexistence steady state of Eq. (20) exists which attracts all trajectories with $Z_1(0) > 0$, $z_2(0) < 1$.*

Remark 4. If there is one steady state satisfying Lemma 6, and any other coexistence steady state with positive Z_1 value is a saddle,

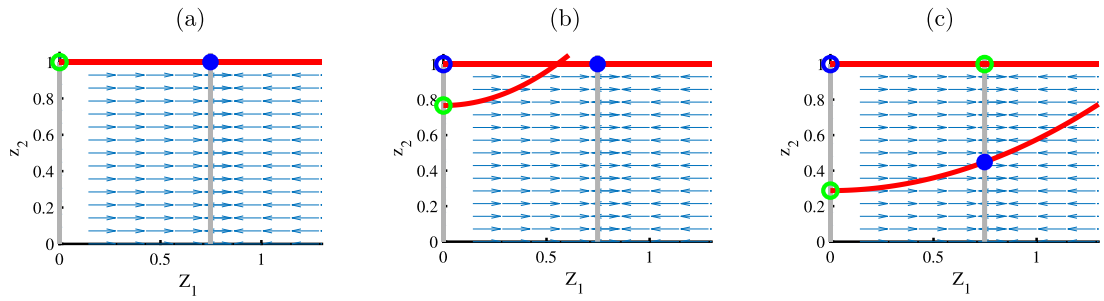

Fig. 7. Phase space for $\beta_2 < 0$ small with increasing numerical value, all other parameters at default values. In (a) $\beta_2 = -2 \cdot 10^{-5}$, in (b) $\beta_2 = -3 \cdot 10^{-5}$, and in (c) $\beta_2 = -8 \cdot 10^{-5}$. As the two null clines cross, a stable coexistence steady state is created, changing the stability of the cancer steady state from stable to unstable. For increasing $|\beta_2|$ the stable equilibrium has decreasing z_2 value. The dynamics is a fast attraction to the stable Z_1 null cline and the slower attraction to the stable coexistence steady state/cancer steady state. As Eq. (47) is independent of β_2, the inner coexistence point (when it exists) moves parallel to the z_2-axis as β_2 is varied.

then there are no closed orbits. This is due to index theory [64] that disallows a closed orbit solely enclosing one or more saddles.

Considering again the necessary condition for a coexistence point $f_1(Z_1) = f_2(Z_1)$ which implies

$$\sqrt{1+\beta_1 Z_1}\left(1-\beta_4\left(1+Z_1^2\right)\right) = \left(\beta_3+\beta_4\right)\left(1+Z_1^2\right) - 1\,. \tag{46}$$

Squaring this expression and collection terms of same order, the Z_1-value at the coexistence point must satisfy a fifth order polynomial

$$\begin{aligned} 0 = &-\alpha_2{\alpha_5}^2 {Z_1}^5 + \left({\alpha_4}^2 + 2\,\alpha_4\alpha_5\right){Z_1}^4 + \left(-2\,\alpha_2{\alpha_5}^2 + 2\,\alpha_2\alpha_5\right){Z_1}^3 \\ &+ \left(2\,{\alpha_4}^2 + 4\,\alpha_4\alpha_5 - 2\,\alpha_4\right){Z_1}^2 + \left(-\alpha_2{\alpha_5}^2 + 2\,\alpha_2\alpha_5 - \alpha_2\right)Z_1 + {\alpha_4}^2 \\ &+ 2\,\alpha_4\alpha_5 - 2\,\alpha_4\,, \end{aligned} \tag{47}$$

with the constraint that Eq. (46) must be valid. Then, the z_2 value at the coexistence point can be computed from Eq. (35). Notice that Eq. (47) is independent of β_2 while Eq. (35) is not. Therefore, perturbing β_2 the coexistence point moves parallel to the z_2 axis, see Fig. 7. Hence, increasing the self renewal of CSC compared to HSC increase the allele burden but not the total blood cell count in this case. The polynomial formulation of the steady state is easily implemented in e.g. Matlab for numerical implementation.

Possible phase planes for $-1 < \beta_2 < 0, \beta_4 > 0, 0 < \beta_3 < 2$ are shown in Fig. 8. The different cases are found by investigating the existence and order of $z_2 = f_1(Z_1)$ and $z_2 = f_2(Z_1)$ crossing each other and the boundaries. We have found no more than two coexistence steady states with positive Z_1 value, for a given parameter set of parameter values.

2.4.8. *The case* $\beta_2 = -1$, $\beta_4 > 0$

This case is similar to $0 > \beta_2 > -1$ except there can be no cancer steady states and hence will not be elaborated further. The possible topologies are shown in Fig. 9.

3. Discussion

A two dimensional model is presented to investigate the dynamics of cancer and hematopoietic stem cells and mature cells, immune system activity, and clearing of dead cells, including a nonlinear niche feedback with competition between the two stem cell types. In the model the self renewal rates for HSC and CSC are allowed to differ while some other parameters being assumed equal for the HSC and CSC dynamics. For a wide range of parameter values, analytical insight in the global dynamics is obtained revealing that the competition at stem cell level, β_2, is crucial for whether hematopoiesis is maintained or MPN dominates. In particular, $\beta_2 > 0$ is a signature of cancer growth out competing healthy hematopoietic cells, while $\beta_2 < 0$ is needed for stable hematopoiesis or a sustained, low cancer burden.

3.1. *Elevated JAK2 in patients without MPN diagnosis*

Blood samples from non MPN diagnosed patients have been analysed by Xu et al. [65] who found that about 1% of the 3935 investigated subjects were *JAK2* positive, with 70% of these having low allele burdens i.e. less than 5%. A general population study found that 0.2% of the population harbours the *JAK2* mutation [66]. In a large Swedish study [22], the number of patients with MPN is found as 3035 during the years 2001 to 2008. With a population size of 9 millions this implies a prevalence of 0.03%.

How can the role of *JAK2* mutation as a driver for cancer development for MPN patients be consistent with many carrying the *JAK2* mutation do not have an MPN diagnosis? One explanation could of course be, that a large number of subjects were in an early, yet undiagnosed state of MPNs.

Traulsen et al. [17] suggest another reason, namely that the *JAK2* mutation found in the study of [65] is not occurring at the stem cell level but further down the proliferation chain hence not affecting hematopoiesis so severely. This would imply that after some time, the *JAK2* positive cells are depleted. However, a small, stable *JAK2* fraction can be maintained for years [67]. Our analysis suggests an alternative answer; the non MPN diagnosed subjects are characterized by parameter values rendering a stable, coexistence point with low allele burden corresponding to Fig. 8(f), (g), (n). Alternatively, the MPN fraction of cells may be slowly increasing corresponding to HSC and CSC selfrenewal being of comparable size. This may be more feasible than multiple *JAK2* mutations in the same individual [68]. Another interesting explanation is the *active immune window* where malignant cells need to reach a critical level before the immune system is activated to keep a low disease level. This has proven a fruitful explanation for describing clinical data of patients with chronic myeloid leukemia [69].

3.2. *Intervention strategies*

From the previous analysis it is clear that the sign of β_2 is important for treatment outcome. Intervention at stem cell level is important to ensure cure or minimal residual disease which is relevant also for chronic myeloid leukemia [40]. In Fig. 11 a model simulation with default parameter values is shown along with median data of two sets of patients with polycythemera vera treated with pegylated interferon-α-2a [70,71]. Altering β_2 by decreasing r_y and increasing r_x corresponds to a mechanism of the drug where the malignant clone is targeted [70,72] and HSC are activated [73]. Only the initial conditions vary, corresponding to a different initial allele burden for each group of study. Hence, by altering β_2 to the value −0.9, two clinical data sets can be reproduced using a single parameter set in the model.

The phase plane dynamics with β_2 having small, negative values are shown in Fig. 7 showing how a stable cancer steady state bifurcates to a stable coexistence steady state when perturbing β_2. In Fig. 12, two treatment scenarios are shown based on changing β_2 from positive

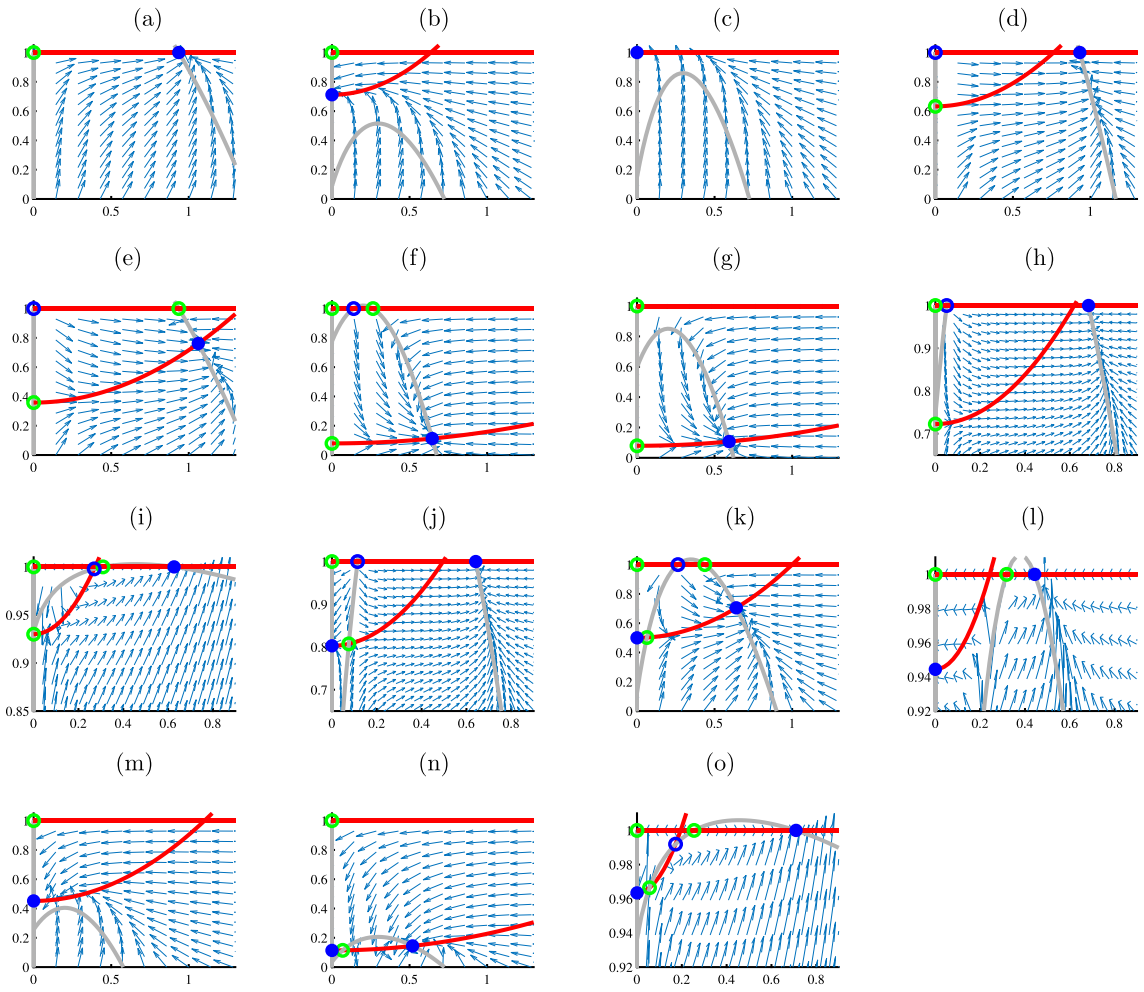

Fig. 8. Phase plane, (Z_1, z_2), for $-1 < \beta_2 < 0$, $\beta_4 > 0$. Corresponding parameter values are listed in Tables 3 and 4. In all cases except (i) and (o), there can be no period orbits, hence the steady states are the only possible attractors. Unhealthy attractors are located on the lines $Z_1 = 0$ and $z_2 = 1$, while a coexistence steady state with positive Z_1 value may be unhealthy or healthy, for example (f), (g), (n) may be considered healthy conditions for most initial conditions.

Table 3
Parameter values for Fig. 8 (a)–(h).

	(a)	(b)	(c)	(d)	(e)	(f)	(g)	(h)
β_1	5	4	4	2	5	2	2	5
β_2	−.2793	−.2793	−.1676	−.1676	−.2793	−.1676	−.1676	−.1816
β_3	1.3	1.95	1.95	1.2	1.3	1.74	1.8	1.73
β_4	.3313	.1988	.2916	.106	.1	.0133	.0133	.8469

Table 4
Parameter values for Fig. 8 (i)–(o).

	(i)	(j)	(k)	(l)	(m)	(n)	(o)
β_1	20	6	6	8	2	4	20
β_2	−.9107	−.1536	−.2000	−.2933	−.2933	−.6984	−.9079
β_3	0.3	1.92	1.95	1.85	1.85	1.95	.3
β_4	.8469	.1233	.1	.2770	.1325	.0795	.8747

to negative values. Starting treatment at a high allele burden can ultimately lead to reversal to a healthy, hematopoietic steady state or a coexistence steady state with low allele burden. An effective drug (high dose) may have the negative impact that the total number of white blood cells have critically low values in the transition from a high allele burden to a healthy state as can be seen by considering the trajectories in Fig. 12. This suggests that maintaining a low dose or slowly increasing dose during treatment may be important, or that treatment should also address other parameters.

Intervention at an early cancer stage is preferred for several reasons for example reducing the risk of thrombosis or hemorrhage. Our phase plane analysis suggests further that an early intervention can lead to a coexistence steady state with low tumour load while late intervention may lead to out competition of healthy cells even though the self renewal of HSC is larger than that of CSC. This may occur when there are three coexistence steady states, for initial conditions with large allele burdens are in the basin of attraction of the stable steady state causing extinction of healthy cells — see Fig. 13. Furthermore, for initial conditions in the basin of attraction of the relatively healthy coexistence steady state, a high initial allele burden implies a transient with a low Z_1 value compared to the steady state. Hence, late treatment start may imply more serious adverse events which advocates for early treatment. The separatrix (black curve) provides a threshold for initial conditions that will maintain homeostasis versus eradicate healthy cells. A similar approach has proven useful for studying the dynamics of Hepatitis C Virus and immune suppression [74].

3.3. Comparison of the simple and full model

The simple model is a good representation of the full model for cancer progression. An important reason for this is the assumption that cancer initiation is a perturbation to a hematopoietic steady state i.e. initially $y_0' = y_1' = a' = s' = 0$ which implies that no transients are observed for the trajectories of the full model to be close to the simple model. Initiating a treatment may be interpreted as a fast change in

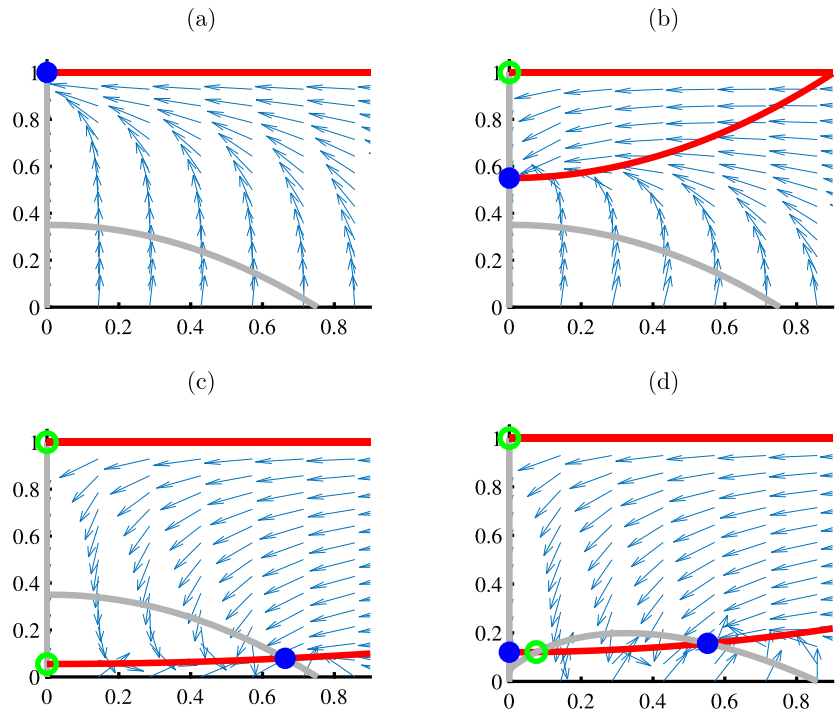

Fig. 9. Phase space for $\beta_2 = -1$. (a) and (b) are unhealthy conditions while (c) and (d) are healthy for most initial conditions.

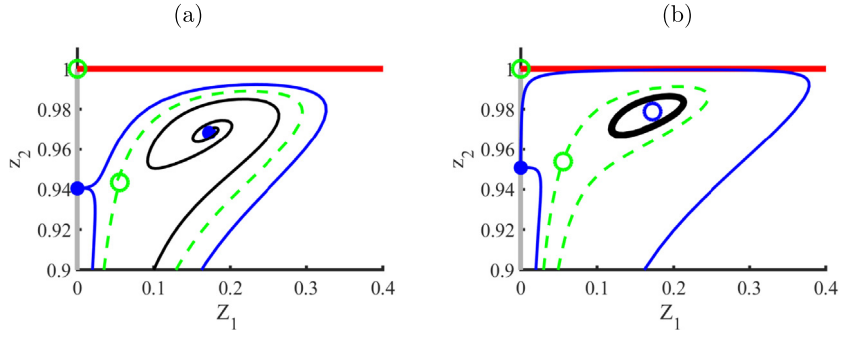

Fig. 10. In (a) there are two stable steady states and two saddles. Selected trajectories are shown in green, blue and black curves. Parameter values are $\beta_1 = 20, \beta_2 = -.93, \beta_3 = .3, \beta_4 = .8747$. In (b) $\beta_2 = -.92$ with the remaining parameter values being the same as in (a). A Hopf-bifurcation has occurred for some $\beta_2 \in (-.92; -.93)$ such that a stable coexistence steady state has turned unstable and a stable limit cycle has appeared.

one or more parameter values. In Fig. 14 the simple and the full model are evolved with default parameter values until an allele burden of 50% is obtained. Then, a parameter value is abruptly changed, and the resulting trajectories of stem cells and mature blood cells are shown for the full and simple model. The simple model is a good approximation to the full model when altering a stem cell parameter value such as r_x or r_y as seen in Fig. 14(a) which supports the use of the simple model in Fig. 11. Changing a parameter value of the mature cells such as d_{x1} leads to a discontinuity in the simple model and a fast transient in the full model, hence for a short time the full model and the reduced model do not match — see 14(b). This discontinuity is expected in the simple model from Eq. (3c); a jump in d_{x1} leads to a jump in x_1. Hence, for treatments mainly affecting mature cells, a fast transient between the full and the reduced model may be observed. The full model and the simple model have exactly the same steady states. However, the stability steady states in a quasi steady state model and a full model may differ. In Fig. 15 a bifurcation diagram is shown for the reduced model by computing steady states and their stability at 500 times 250 grid points. Likewise, the corresponding steady state of the full model can be investigated by fixing all full model parameters at default values except r_m, r_y, e_s and r_s that can be computed from the values of $\beta_1, \beta_2, \beta_3$ and β_4 by inverting Eq. (21). Then, the stability of the full model is assessed by the dominant eigenvalue of the six by six dimensional Jacobian. The stability of the full model and simple model are found to be identical everywhere.

3.4. Early MPN phase

One hit mutation

Assuming little change in Z_1 in the early cancer phase, we may derive expressions for cancer growth for a one hit mutation, i.e. $\beta_4 = 0$. In that case

$$\dot{z}_2 = k_1 \beta_2 \left(1 - z_2\right) z_2 \,, \tag{48}$$

with $k_1 = \frac{1+\sqrt{1+\beta_1 Z_1}}{1+Z_1^2}$ and with the initial condition being a positive, small allele burden, z_{20} at time equal to zero. This equation may be solved providing the well known expression for logistic growth. Such an expression is well known in cancer descriptions. However, the approach here with the logistic growth as an asymptotic case of a more elaborate model allows for inferring mechanisms to the parameters of the one dimensional model Eq. (48). Thus, in the early cancer phase, if the

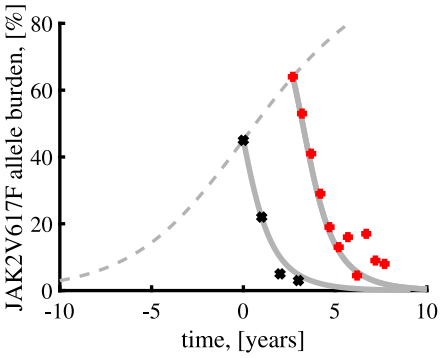

Fig. 11. Grey stipulated curve is cancer growth using the default parameter values in the simple model shifted in time such that the *JAK2* allele burden is 45% at $t = 0$. Dots are median values from two independent clinical studies of patients with polycythemia vera treated with pegylated interferon-α-2a. Red dots are from [70] (43 patients), black dots are from [71] (40 patients). Full grey curves are output of the simple model, with $\beta_2 = -.9$, which is obtained by a doubling in r_x as interferon increases stem cell activity [73] and a reduction in r_y. Remaining parameters set to default values. The only difference between the two grey curves is the initial conditions. Hence, the simple model with a unique set of parameter values can reproduce several clinical reports on PV patients with the explained effect being related to increased HSC function compared to CSC during treatment.

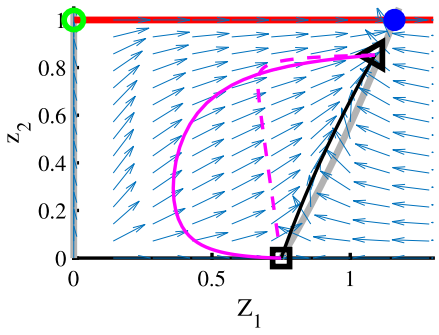

Fig. 12. Phase space with default parameter values where the full blown MPN cancer is the stable steady state. A typical trajectory (black curve) is shown with initial condition in the black square. A successful treatment must change the sign of β_2 from positive to negative. At the triangle, two different treatments are initiated (magenta), for the full curves $\beta_2 = -0.9$ and for the dashed $\beta_2 = -0.1$. The temporary, small value of Z_1 at the full, magenta curve suggests that an effective treatment may reduce the number of white blood cells too severely. However, a more gradual change of β_2 corresponding to a slowly increasing dose of an effective drug does not have the same shortcoming.

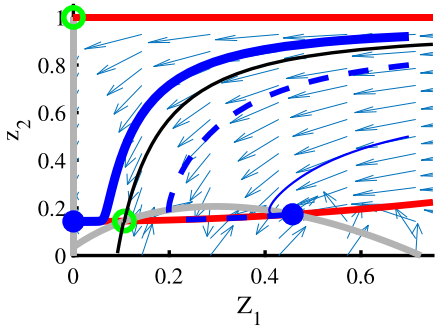

Fig. 13. Possible phase plane for $\beta_2 < 0, \beta_4 > 0$. Blue curves are specific trajectories. Black curves are the stable manifolds of the saddle point (green circle) dividing the phase space in two bassins of attraction. In the right region the stable, coexistence point is a relatively healthy state while the left region implies extinction of healthy cells for any initial condition. The case showed here may be a result of intervention with $\beta_2 > 0$ prior to intervention and $\beta_2 < 0$ after intervention. Early intervention leads to an initial condition in the lower right part of the phase space which corresponds to a non expanding malignant cell count i.e. a relatively healthy condition. The thick blue curve shows that the same intervention at large, initial malignant cell counts can lead to eradication of healthy cells.

disease is diagnosed and treatment is conducted, which change the sign of β_2 from positive to negative with new value denoted $\hat{\beta}_2$, then, disease progression is changed from logistic growth to logistic decay. However, the dose–response relation may be unknown. Comparing the growth curve at allele burden, z_2 before treatment to allele burden $\hat{z}_2$ after treatment using the lab time t we observe

$$\frac{z_2'}{\hat{z}_2'} = \frac{\beta_2 \left(1 - z_2\right) z_2}{\hat{\beta}_2 \left(1 - \hat{z}_2\right) \hat{z}_2}. \tag{49}$$

This means that the change in stem cell parameters, $\frac{\beta_2}{\hat{\beta}_2}$ can be directly computed from considering the slope of allele burden of mature cells prior to and after treatment without use of sophisticated parameter estimation techniques. In this way, mathematical modelling and reasoning give a window to investigate the hardly accessible stem cell dynamics by mechanistic modelling and measurements of the mature cells.

Solving (48) with a change of β_2 value to another value $\hat{\beta}_2$ at time $\tau = T$ gives

$$z_2(\tau) = \frac{z_{20} e^{\beta_2 k_1 \tau}}{z_{20}\left(e^{\beta_2 k_1 \tau} - 1\right) + 1}, \qquad \text{for} \quad 0 \le \tau \le T \tag{50a}$$

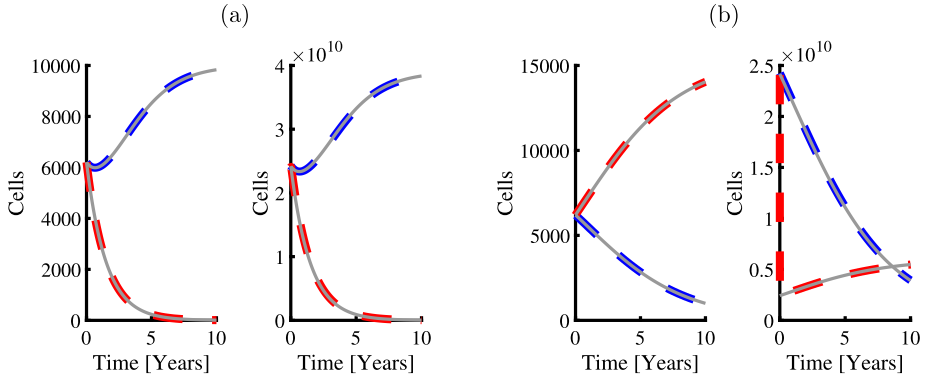

Fig. 14. Initial conditions correspond to integrating the full or simple model with default parameter values until equal amounts of hematopoietic and cancer stem cells. Then, an abrupt change in a parameter value is applied, representing a potential treatment. In (a) β_2 is changed to $-.9$ by reducing r_y and doubling r_x which correspond to the suggested effect of pegylated interferon-α-2a in Fig. 11. Left panel is stem cell numbers, right panel is mature cell numbers. Blue curves are hematopoietic cells, red are blood cancer cells. Grey curves are the corresponding trajectories from the simple model. For an abrupt change in stem cell parameters, the simple model, (3) remains a good approximation to the full model (1). In (b) the value of d_{y1} is increased by a factor 10 with the remaining parameters at default value. Here, the mature cancer cell count drops immediately in the simple model while the full model has a fast transient before good agreement again is observed between the full model and the two dimensional model. Though an increased death rate of mature, cancer cells implies an immediate reduction of mature cancer cells, the mature hematopoietic cells are not restored by this intervention and in the long run, the mature cancer cells again dominate the mature hematopoietic cells i.e. this intervention does not provide a cure.

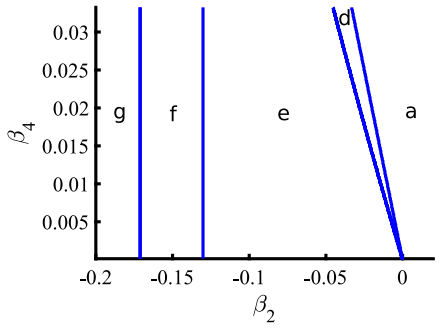

Fig. 15. Bifurcation diagram, with $\beta_1 = 2$, $\beta_3 = 1.74$ and varying β_2 and β_4. The letters on the figure correspond to the topologies in Fig. 8, hence showing possible transitions between the topologies as parameters are perturbed. In regions g, f, e the stable steady state is a coexistence steady state, while in regions d and a a cancer steady state is the only stable steady state.

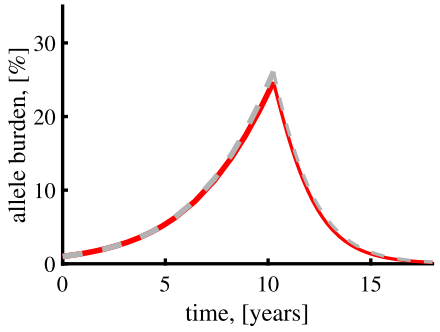

Fig. 16. Red, thick curve is allele burden growth using the simple, reduced model with default parameters. At year 10, a treatment intervention changes the β_2 value to −0.9 showed by the thin red, solid line. Grey curves are the corresponding analytic approximation given by Eq. (50) with $z_2(0) = 0.01$ corresponding to the sensitivity of the best assays.

$$\hat{z}_2(\tau) = \frac{z_2(T)e^{\hat{\beta}_2 k_1(\tau-T)}}{z_2(T)\left(e^{\hat{\beta}_2 k_1(\tau-T)} - 1\right) + 1}, \quad \text{for} \quad \tau > T \tag{50b}$$

A comparison of this formula to the simple, reduced model is seen in Fig. 16 providing a good approximation within the measurable, low allele burden regime.

3.5. Role of exogenous inflammation stimuli

We reformulate Eq. (50) in terms of the original parameters

$$z_2(t) = \frac{z_{20}e^{\gamma t}}{z_{20}\left(e^{\gamma t} - 1\right) + 1}, \qquad \text{for} \quad 0 \le t \le \hat{T} \tag{51a}$$

$$z_2(t) = \frac{z_2(\hat{T})e^{\hat{\gamma}(t-\hat{T})}}{z_2(\hat{T})\left(e^{\hat{\gamma}(t-\hat{T})} - 1\right) + 1}, \quad \text{for} \quad t > \hat{T} \tag{51b}$$

with

$$\gamma = \frac{r_y - r_x}{2e_s\left(1 + \bar{Z}_1^2\right)}\left(I + \sqrt{I^2 + \left(4\frac{e_s r_s}{c_{xx}e_a}\left(a_x A_x + d_{x0}\right)\right)\bar{Z}_1}\right). \tag{52}$$

This implies $|\gamma|$ increases with I, i.e. disease progression is accelerated for a large endogenous inflammatory stimuli, when $r_y > r_x$. Surprisingly, in case an intervention happens, such that $r_y > r_x$ prior to treatment but $r_x > r_y$ after treatment, then inflammation acts as a disease driver prior to treatment but after treatment inflammation acts like a health promoter. Similarly, one may predict the behaviour of perturbing the original parameters $e_s, r_s, c_{xx}, e_a, a_x, A_x, d_{x0}$.

Declaration of competing interest

The authors declare that they have no known competing financial interests or personal relationships that could have appeared to influence the work reported in this paper.

Appendix. Derivation of the simple cancitis model

Model (1) is written here again for convenience

$$x_0' = \left(r_x\phi_x s - d_{x0} - a_x\right)x_0 - r_m s x_0 \tag{53a}$$

$$x_1' = a_x A_x x_0 - d_{x1}x_1 \tag{53b}$$

$$y_0' = \left(r_y\phi_y s - d_{y0} - a_y\right)y_0 + r_m s x_0 \tag{53c}$$

$$y_1' = a_y A_y y_0 - d_{y1}y_1 \tag{53d}$$

$$a' = d_{x0}x_0 + d_{y0}y_0 + d_{x1}x_1 + d_{y1}y_1 - e_a a s \tag{53e}$$

$$s' = r_s a - e_s s + I(t) \tag{53f}$$

$$\phi_x = \phi_x(x_0, y_0) = \frac{1}{1 + \left(c_{xx}x_0 + c_{xy}y_0\right)^2} \tag{53g}$$

$$\phi_y = \phi_x(x_0, y_0) = \frac{1}{1 + \left(c_{yx}x_0 + c_{yy}y_0\right)^2} \tag{53h}$$

These equations are subject to a quasi steady state assumption of all compartments except the stem cells

$$x_1' = y_1' = a' = s' = 0, \tag{54}$$

and with constant I. From $x_1' = 0$, x_1 is easily expressed as

$$x_1 = \frac{a_x A_x}{d_{x1}}x_0, \tag{55}$$

and similarly $y_1' = 0$ implies

$$y_1 = \frac{a_y A_y}{d_{y1}}y_0. \tag{56}$$

From $s' = 0$ we get

$$a = \frac{e_s}{r_s}s - \frac{I}{r_s} \tag{57}$$

Inserting this in Eq. (53e) with $a' = 0$ we arrive at

$$0 = d_{x0}x_0 + d_{y0}y_0 + d_{x1}x_1 + d_{y1}y_1 - e_a s\left(\frac{e_s}{r_s}s - \frac{I}{r_s}\right) \tag{58}$$

which may be considered a second order polynomial in s. Solving for the roots we get

$$s_\pm = \frac{I}{2e_s} \pm \sqrt{\left(\frac{I}{2e_s}\right)^2 + \frac{r_s}{e_s e_a}\left(d_{x0}x_0 + d_{y0}y_0 + d_{x1}x_1 + d_{y1}y_1\right)} \tag{59}$$

As we are only interested in non negative s values, only $s = s_+$ is kept and Eqs. (55) and (56) are inserted to give

$$s = \frac{I}{2e_s} + \sqrt{\left(\frac{I}{2e_s}\right)^2 + \frac{r_s\left(a_x A_x + d_{x0}\right)}{e_a e_s}\left(x_0 + \frac{a_y A_y + d_{y0}}{a_x A_x + d_{x0}}y_0\right)} \tag{60}$$

Inserting this expression for s in Eq. (57) provides a as a function of x_0 and y_0

$$a = -\frac{I}{2r_s} + \frac{e_s}{r_s}\sqrt{\left(\frac{I}{2e_s}\right)^2 + \frac{r_s\left(a_x A_x + d_{x0}\right)}{e_a e_s}\left(x_0 + \frac{a_y A_y + d_{y0}}{a_x A_x + d_{x0}}y_0\right)} \tag{61}$$

Differential equations (53a) and (53c) together with the algebraic equations (55), (56), (59) and (61) constitute the simple cancitis model.

References

[1] I.R. Lemischka, D.H. Raulet, R.C. Mulligan, Developmental potential and dynamic behavior of hematopoietic stem cells, Cell 45 (6) (1986) 917–927, http://dx.doi.org/10.1016/0092-8674(86)90566-0.

[2] S.N. Catlin, L. Busque, R.E. Gale, P. Guttorp, J.L. Abkowitz, The replication rate of human hematopoietic stem cells in vivo, Blood 117 (17) (2011) 4460–4466, http://dx.doi.org/10.1182/blood-2010-08-303537.The, http://bloodjournal.hematologylibrary.org/content/117/17/4460.short.

[3] H. Lee-Six, N.F. Øbro, M.S. Shepherd, S. Grossmann, K. Dawson, M. Belmonte, R.J. Osborne, B.J.P. Huntly, I. Martincorena, E. Anderson, L. O'Neill, M.R. Stratton, E. Laurenti, A.R. Green, D.G. Kent, P.J. Campbell, Population dynamics of normal human blood inferred from somatic mutations, Nature 561 (7724) (2018-09-01) 473,478, http://search.proquest.com/docview/2100329539/.

[4] H. Vaziri, W. Dragowska, R.C. Allsopp, T.E. Thomas, C.B. Harley, P.M. Lansdorp, Evidence for a mitotic clock in human hematopoietic stem cells: Loss of telomeric DNA with age, Proc. Natl. Acad. Sci. 91 (21) (1994) 9857–9860, http://dx.doi.org/10.1073/pnas.91.21.9857.

[5] M.C. Mackey, Cell kinetic status of haematopoietic stem cells, Cell Prolif. 34 (2) (2001) 71–83, http://dx.doi.org/10.1046/j.1365-2184.2001.00195.x.

[6] P. Getto, A. Marciniak-Czochra, Y. Nakata, M.d. Vivanco, Global dynamics of two-compartment models for cell production systems with regulatory mechanisms, Math. Biosci. 245 (2) (2013) 258–268, http://dx.doi.org/10.1016/j.mbs.2013.07.006.

[7] T. Stiehl, A. Marciniak-Czochra, P. Greulich, B. MacArthur, Stem cell self-renewal in regeneration and cancer: Insights from mathematical modeling, Curr. Opin. Syst. Biol. 5 (2017) 112–120, http://dx.doi.org/10.1016/j.coisb.2017.09.006.

[8] A. Marciniak-Czochra, T. Stiehl, A.D. Ho, W. Jäger, W. Wagner, Modeling of asymmetric cell division in hematopoietic stem cells–regulation of self-renewal is essential for efficient repopulation, Stem cells Develop. 18 (3) (2009) 377–385, http://dx.doi.org/10.1089/scd.2008.0143, arXiv:arXiv:1011.1669v3.

[9] E. Manesso, J. Teles, D. Bryder, C. Peterson, Dynamical modelling of haematopoiesis: An integrated view over the system in homeostasis and under perturbation, J. R. Soc. Interface 10 (80) (2013) 20120817, http://dx.doi.org/10.1098/rsif.2012.0817, http://www.ncbi.nlm.nih.gov/pubmed/23256190.

[10] Z. Sajid, M. Andersen, J.T. Ottesen, Mathematical analysis of the cancitis model and the role of inflammation in blood cancer progression, Math. Biosci. Eng. 16 (6) (2019) 8268–8289, http://dx.doi.org/10.3934/mbe.2019418.

[11] S. Rubinow, J. Lebowitz, A mathematical model of neutrophil production and control in normal man, J. Math. Biol. 1 (3) (1975) 187–225.

[12] J. Lei, M.C. Mackey, Multistability in an age-structured model of hematopoiesis: Cyclical neutropenia, J. Theoret. Biol. 270 (1) (2011) 143–153, http://dx.doi.org/10.1016/j.jtbi.2010.11.024.

[13] T. Hillen, H. Enderling, P. Hahnfeldt, The tumor growth paradox and immune system-mediated selection for cancer stem cells, Bull. Math. Biol. 75 (1) (2013) 161–184, http://dx.doi.org/10.1007/s11538-012-9798-x.

[14] L. Berezansky, E. Braverman, L. Idels, Mackey-Glass model of hematopoiesis with monotone feedback revisited, Appl. Math. Comput. 219 (9) (2013) 4892–4907, http://dx.doi.org/10.1016/j.amc.2012.10.052.

[15] D. Dingli, A. Traulsen, F. Michor, (A) symmetric stem cell replication and Cancer, PLoS Comput. Biol. 3 (3) (2007) 30083, http://dx.doi.org/10.1371/journal.pcbi.0030053.

[16] D. Dingli, J.M. Pacheco, Stochastic dynamics and the evolution of mutations in stem cells, BMC Biol. 9 (41) (2011) 1–7.

[17] A. Traulsen, J.M. Pacheco, L. Luzzatto, D. Dingli, Somatic mutations and the hierarchy of hematopoiesis, BioEssays 32 (11) (2010) 1003–1008, http://dx.doi.org/10.1002/bies.201000025.

[18] N.L. Komarova, Principles of regulation of self-renewing cell lineages, PLoS One 8 (9) (2013) 1–12, http://dx.doi.org/10.1371/journal.pone.0072847.

[19] M.A. Böttcher, D. Dingli, B. Werner, A. Traulsen, Replicative cellular age distributions in compartmentalized tissues, J. R. Soc. Interface 15 (145) (2018-08-01) http://search.proquest.com/docview/2097590395/.

[20] M. Doumic, A. Marciniak-Czochra, B. Perthame, J. Zubelli, A structured population model of cell differentiation, SIAM J. Appl. Math. 71 (6) (2011) 1918–1940, http://search.proquest.com/docview/2085628295/.

[21] P. Ashcroft, M.G. Manz, S. Bonhoeffer, Clonal dominance and transplantation dynamics in hematopoietic stem cell compartments, PLoS Comput. Biol. 13 (10) (2017) 1–20.

[22] M. Hultcrantz, M. Björkholm, P.W. Dickman, O. Landgren, A.R. Derolf, S.Y. Kristinsson, T.M. Andersson, Risk for arterial and venous thrombosis in patients with myeloproliferative neoplasms: A population-based cohort study , Ann. Internal Med. 168 (5) (2018) 317–325, http://dx.doi.org/10.7326/M17-0028.

[23] A.L. MacLean, S. Filippi, M.P.H. Stumpf, The ecology in the hematopoietic stem cell niche determines the clinical outcome in chronic myeloid leukemia, Proc. Natl. Acad. Sci. 111 (10) (2014) 3883–3888, http://dx.doi.org/10.1073/pnas.1317072111.

[24] T. Stiehl, A.D. Ho, A. Marciniak-Czochra, Mathematical modeling of the impact of cytokine response of acute myeloid leukemia cells on patient prognosis, Sci. Rep. 8 (1) (2018) 1–11, http://dx.doi.org/10.1038/s41598-018-21115-4.

[25] T. Stiehl, A. Marciniak-Czochra, Mathematical modeling of leukemogenesis and cancer stem cell dynamics, Math. Model. Nat. Phenom. 7 (1) (2012) 166–202, http://dx.doi.org/10.1051/mmnp/20127199.

[26] A. Besse, G.D. Clapp, S. Bernard, F.E. Nicolini, D. Levy, T. Lepoutre, Stability analysis of a model of interaction between the immune system and cancer cells in chronic myelogenous leukemia, Bull. Math. Biol. 80 (2018) 1084–1110, http://dx.doi.org/10.1007/s11538-017-0272-7.

[27] A. Eladdadi, P. Kim, D. Mallet, Mathematical Models of Tumor- Immune System Dynamics, Springer, New York, 2016.

[28] H. Enderling, Cancer stem cells: Small subpopulation or evolving fraction? Integr. Biol. 7 (1) (2014) 14–23, http://dx.doi.org/10.1039/c4ib00191e, http://pubs.rsc.org/en/Content/ArticleHTML/2015/IB/C4IB00191E.

[29] P.S. Kim, P.P. Lee, D. Levy, A PDE model for imatinib-treated chronic myelogenous leukemia, Bull. Math. Biol. 70 (7) (2008) 1994–2016, http://dx.doi.org/10.1007/s11538-008-9336-z.

[30] N.L. Komarova, D. Wodarz, Effect of cellular quiescence on the success of targeted CML therapy, PLoS One (2007) http://dx.doi.org/10.1371/journal.pone.0000990.

[31] F. Michor, T.P. Hughes, Y. Iwasa, S. Branford, N.P. Shah, C.L. Sawyers, M.A. Nowak, Dynamics of chronic myeloid leukaemia, Nature 435 (June) (2005) 1267–1270, http://dx.doi.org/10.1038/nature03669, arXiv:/status.nature.com/.

[32] F. Michor, Mathematical models of cancer stem cells, J. Clin. Oncol. 26 (17) (2008) 2854–2861, http://dx.doi.org/10.1200/JCO.2007.15.2421.

[33] I.A. Rodriguez-Brenes, N.L. Komarova, D. Wodarz, Evolutionary dynamics of feedback escape and the development of stem-cell-driven cancers, Proc. Natl. Acad. Sci. 108 (47) (2011) 18983–18988, http://dx.doi.org/10.1073/pnas.1107621108.

[34] I. Roeder, M. Horn, Glauche, A. Hochhaus, M. Mueller, M. Loeffler, Dynamic modeling of imatinib treated chronic myeloid leukemia: Functional insights and clinical implications, Nat. Med. 12 (2006) 1181–1184.

[35] J.L. Spivak, The myeloproliferative neoplasms, New Engl. J. Med. 376 (2017) 2168–2181.

[36] J. Zhang, A.G. Fleischman, D. Wodarz, N.L. Komarova, Determining the role of inflammation in the selection of JAK2 mutant cells in myeloproliferative neoplasms, J. Theoret. Biol. (2017) http://dx.doi.org/10.1016/j.jtbi.2017.05.012.

[37] M. Andersen, Z. Sajid, R.K. Pedersen, J. Gudmand-Høeyer, C. Ellervik, V. Skov, L. Kjær, N. Pallisgaard, T.A. Kruse, M. Thomassen, J. Troelsen, H.C. Hasselbalch, J.T. Ottesen, Mathematical modelling as a proof of concept for MPNs as a human inflammation model for cancer development, PLoS One 12 (8) (2017) 1–18, http://dx.doi.org/10.1371/journal.pone.0183620.

[38] J.T. Ottesen, R.K. Pedersen, Z. Sajid, J. Gudmand-Høyer, K.O. Bangsgaard, V. Skov, L. Kjær, T.A. Knudsen, N. Pallisgaard, H.C. Hasselbalch, M. Andersen, Bridging blood cancers and inflammation: The reduced cancitis model, J. Theoret. Biol. 465 (2019) 90–108, http://dx.doi.org/10.1016/j.jtbi.2019.01.001, http://www.sciencedirect.com/science/article/pii/S0022519319300013.

[39] T. Stiehl, A. Marciniak-Czochra, Characterization of stem cells using mathematical models of multistage cell lineages, Math. Comput. Modelling 53 (7) (2011) 1505–1517, http://dx.doi.org/10.1016/j.mcm.2010.03.057, http://www.sciencedirect.com/science/article/pii/S0895717710001755.

[40] D. Dingli, F. Michor, Successful therapy must eradicate cancer stem cells, Stem Cells 24 (12) (2006) 2603–2610.

[41] T. Stiehl, N. Baran, A.D. Ho, A. Marciniak-Czochra, Cell division patterns in acute myeloid leukemia stem-like cells determine clinical course: A model to predict patient survival, Cancer Res. 75 (6) (2015) 940–949, http://dx.doi.org/10.1158/0008-5472.CAN-14-2508.

[42] K.Y. King, M.A. Goodell, Inflammatory modulation of HSCs: viewing the HSC as a foundation for the immune response, Nat. Rev. Immunol. 11 (10) (2011-09-09) 685–692.

[43] H.C. Hasselbalch, M. Bjørn, MPNS as inflammatory diseases: The evidence, consequences, and perspectives, Mediators Inflamm. (2015) 1–16, http://dx.doi.org/10.1155/2015/102476.

[44] H.C. Hasselbalch, A role of NF-E2 in chronic inflammation and clonal evolution in essential thrombocythemia, polycythemia vera and myelofibrosis? Leuk. Res. 38(2) (2014) 263–266, http://dx.doi.org/10.1016/j.leukres.2013.07.002.

[45] C. Desterke, C. Martinaud, N. Ruzehaji, M.C. Le Bousse-Kerdilés, Inflammation as a keystone of bone marrow stroma alterations in primary myelofibrosis, Mediators Inflamm. 2015 (2015) 16, http://dx.doi.org/10.1155/2015/415024.

[46] B.M. Craver, K. El Alaoui, R.M. Scherber, A.G. Fleischman, The critical role of inflammation in the pathogenesis and progression of myeloid malignancies, Cancers 10 (4) (2018-04-03) http://search.proquest.com/docview/2021729698/.

[47] S. Koschmieder, T. Mughal, H.C. Hasselbalch, G. Barosi, P. Valent, J.-J. Kiladjian, G. Jeryczynski, H. Gisslinger, J. Jutzi, J. Pahl, R. Hehlmann, A. Vannucchi, F. Cervantes, R. Silver, T. Barbui, Myeloproliferative neoplasms and inflammation: Whether to target the malignant clone or the inflammatory process or both, Leukemia 30(5) (2016) 1018–1024, http://dx.doi.org/10.1038/leu.2016.12.

[48] S. Hermouet, E. Bigot-Corbel, B. Gardie, Pathogenesis of myeloproliferative neoplasms: Role and mechanisms of chronic inflammation, Mediators Inflamm. (2015) 1–16, http://dx.doi.org/10.1155/2015/145293.

[49] K. Wilkie, Systems Biology of Tumor Dormancy. Chapter 10. A review of mathematical models of cancer-immune interactions in the context of tumor dormancy, Advances in Experimental Medicine and Biology, 734, Springer-Verlag, New York, 2013, pp. 201–234, http://dx.doi.org/10.1007/978-1-4614-1445-2, arXiv:978-1-4614-1445-2.

[50] E. Voit, A First Course in System Biology, Garland Science, Taylor & Francis Group, New York and London, 2013.

[51] D. Wodarz, N. Komarova, Dynamics of Cancer. Mathematical Foundations of Oncology, World Scientific Publishing, 2014, pp. 1–514.

[52] H.C. Hasselbalch, Perspectives on chronic inflammation in essential thrombocythemia, polycythemia vera, and myelofibrosis: Is chronic inflammation a trigger and driver of clonal evolution and development of accelerated atherosclerosis and second cancer? Blood 119 (2012) 3219–3225.

[53] H.C. Hasselbalch, Chronic inflammation as a promotor of mutagenesis in essential thrombocythemia, polycythemia vera and myelofibrosis. A human inflammation model for cancer development? Leuk. Res. 37 (2) (2013) 214–220, http://search.proquest.com/docview/1273496450/.

[54] H. Haeno, R.L. Levine, D.G. Gilliland, F. Michor, A progenitor cell origin of myeloid malignancies, Proc. Natl. Acad. Sci. (2009) http://dx.doi.org/10.1073/pnas.0908107106.

[55] S. Gentry, T. Jackson, A mathematical model of Cancer stem cell driven tumor initiation: Implications of niche size and loss of homeostatic regulatory mechanisms, PLoS One 8 (8) (2013) e71128, http://search.proquest.com/docview/1500795341/.

[56] T. Stiehl, C. Lutz, A. Marciniak-Czochra, Emergence of heterogeneity in acute leukemias, Biol. Direct 11 (1) (2016-10-12) 51.

[57] J. Pillay, I. den Braber, N. Vrisekoop, L.M. Kwast, R.J. de Boer, J.A.M. Borghans, K. Tesselaar, L. Koenderman, In vivo labeling with 2H2O reveals a human neutrophil lifespan of 5.4 days, Blood 116 (4) (2010) 625–627, http://dx.doi.org/10.1182/blood-2010-01-259028, arXiv:https://ashpublications.org/blood/article-pdf/116/4/625/1332527/zh803010000625.pdf.

[58] A. Lindholm Sørensen, H.C. Hasselbalch, Smoking and philadelphia-negative chronic myeloproliferative neoplasms, Eur. J. Haematol. 97 (1) (2016) 63–69, http://dx.doi.org/10.1111/ejh.12684.

[59] H.C. Hasselbalch, Smoking as a contributing factor for development of polycythemia vera and related neoplasms, Leuk. Res. 39 (11) (2015-11) 1137,1145.

[60] P.R. Wheater, Functional Histology: A Text and Colour Atlas, second ed., Churchill Livingstone., Edinburgh, 1987.

[61] D. Dingli, J.M. Pacheco, Modeling the architecture and dynamics of hematopoiesis, Wiley Interdiscip. Rev. Syst. Biol. Med. 2 (2010) 235–244, http://dx.doi.org/10.1002/wsbm.56.

[62] C. Robinson, Dynamical Systems, Stability, Symbolic Dynamics, and Chaos, second ed., in: Studies in advanced mathematics, CRC Press, Boca Raton, Fla, 1999.

[63] S. Rao, Stability analysis of the Michaelis - Menten approximation of a mixed mechanism of a phosphorylation system, Math. Biosci. 301 (2018) 159–166, http://dx.doi.org/10.1016/j.mbs.2018.05.001, http://www.sciencedirect.com/science/article/pii/S0025556417306909.

[64] J.D. Meiss, Differentiable Dynamical Systems, first ed., SIAM, 2007.

[65] X. Xu, Q. Zhang, J. Luo, S. Xing, Q. Li, S.B. Krantz, X. Fu, Z.J. Zhao, JAK2V617F: Prevalence in a large Chinese hospital population, Blood 109 (1) (2007) 339–342, http://dx.doi.org/10.1182/blood-2006-03-009472, arXiv:http://www.bloodjournal.org/content/109/1/339.full.pdf.

[66] C. Nielsen, H.S. Birgens, B.G. Nordestgaard, L. Kjær, S.E. Bojesen, The JAK2 V617F somatic mutation, mortality and cancer risk in the general population, Haematologica 96 (3) (2011) 450–453, http://dx.doi.org/10.3324/haematol.2010.033191, arXiv:http://www.haematologica.org/content/96/3/450.full.pdf.

[67] R.E. Gale, A.J.R. Allen, M.J. Nash, D.C. Linch, Long-term serial analysis of X-chromosome inactivation patterns and JAK2 V617F mutant levels in patients with essential thrombocythemia show that minor mutant-positive clones can remain stable for many years, Blood 109 (3) (2007-02-01) 1241,1243, http://search.proquest.com/docview/68945790/.

[68] P. Lundberg, A. Karow, R. Nienhold, R. Looser, H. Hao-Shen, I. Nissen, S. Girsberger, T. Lehmann, J. Passweg, M. Stern, C. Beisel, R. Kralovics, R.C. Skoda, Clonal evolution and clinical correlates of somatic mutations in myeloproliferative neoplasms, Blood 123 (14) (2014-04-03) 2220,2228, http://search.proquest.com/docview/1513051039/.

[69] G.D. Clapp, T. Lepoutre, R. El Cheikh, S. Bernard, J. Ruby, H. Labussière-Wallet, F.E. Nicolini, D. Levy, Implication of the autologous immune system in BCR-ABL transcript variations in chronic myelogenous leukemia patients treated with imatinib, Cancer Res. 75 (19) (2015) 4053–4062, http://search.proquest.com/docview/1718908194/.

[70] A. Quintás-Cardama, O. Abdel-Wahab, T. Manshouri, O. Kilpivaara, J. Cortes, A.-L. Roupie, S.-J. Zhang, D. Harris, Z. Estrov, H. Kantarjian, R.L. Levine, S. Verstovsek, Molecular analysis of patients with polycythemia vera or essential thrombocythemia receiving pegylated interferon alpha-2a, Blood 122 (6) (2013) 893–901, http://dx.doi.org/10.1182/blood-2012-07-442012.

[71] J.-J. Kiladjian, B. Cassinat, S. Chevret, P. Turlure, N. Cambier, M. Roussel, S. Bellucci, B. Grandchamp, C. Chomienne, P. Fenaux, Pegylated interferon-alfa-2a induces complete hematologic and molecular responses with low toxicity in polycythemia vera, Blood 112 (8) (2008) 3065–3072.

[72] J.-J. Kiladjian, S. Giraudier, B. Cassinat, Interferon-alpha for the therapy of myeloproliferative neoplasms: Targeting the malignant clone, Leukemia 30 (4) (2016) 776–781.

[73] M.A.G. Essers, S. Offner, W.E. Blanco-Bose, Z. Waibler, U. Kalinke, M.A. Duchosal, A. Trumpp, IFN Alpha activates dormant haematopoietic stem cells in vivo, Nature 458 (7240) (2009) 904–908.

[74] N.L. Komarova, E. Barnes, P. Klenerman, D. Wodarz, Boosting immunity by antiviral drug therapy: A simple relationship among timing, efficacy, and success, Proc. Natl. Acad. Sci. 100 (4) (2003) 1855–1860, http://dx.doi.org/10.1073/pnas.0337483100, arXiv:https://www.pnas.org/content/100/4/1855.full.pdf.